

# Nanofluid Formulations Based on Two-Dimensional Nanoparticles, Their Performance, and Potential Application as Water-Based Drilling Fluids

Camilo Zamora-Ledezma,\* Christian Narváez-Muñoz, Víctor H. Guerrero, Ernesto Medina, and Luis Meseguer-Olmo



Cite This: *ACS Omega* 2022, 7, 20457–20476

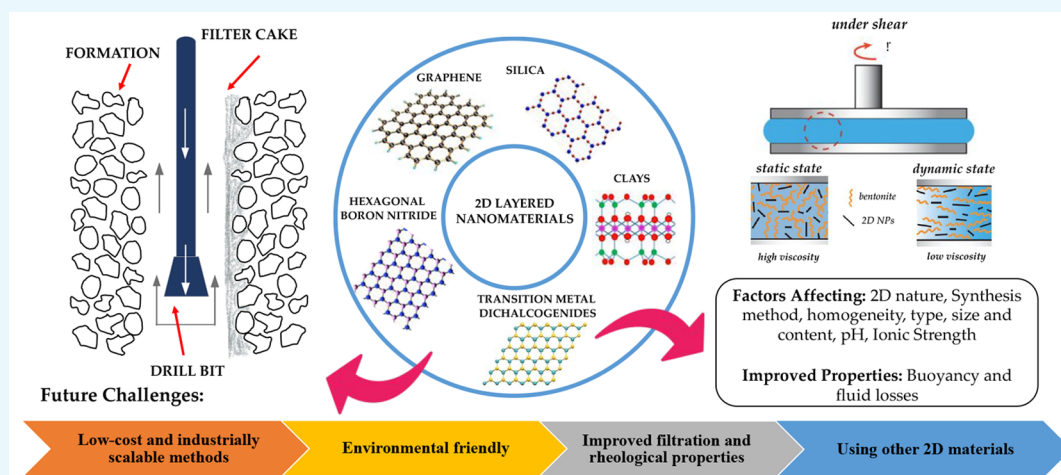


Read Online

ACCESS |

Metrics & More

Article Recommendations



**ABSTRACT:** The development of sustainable, cost-efficient, and high-performance nanofluids is one of the current research topics within drilling applications. The inclusion of tailorable nanoparticles offers the possibility of formulating water-based fluids with enhanced properties, providing unprecedented opportunities in the energy, oil, gas, water, or infrastructure industries. In this work, the most recent and relevant findings related with the development of customizable nanofluids are discussed, focusing on those based on the incorporation of 2D (two-dimensional) nanoparticles and environmentally friendly precursors. The advantages and drawbacks of using 2D layered nanomaterials including but not limited to silicon nano-glass flakes, graphene, MoS<sub>2</sub>, disk-shaped Laponite nanoparticles, layered magnesium aluminum silicate nanoparticles, and nanolayered organo-montmorillonite are presented. The current formulation approaches are listed, as well as their physicochemical characterization: rheology, viscoelastic properties, and filtration properties (fluid losses). The most influential factors affecting the drilling fluid performance, such as the pH, temperature, ionic strength interaction, and pressure, are also debated. Finally, an overview about the simulation at the microscale of fluids flux in porous media is presented, aiming to illustrate the approaches that could be taken to supplement the experimental efforts to research the performance of drilling muds. The information discussed shows that the addition of 2D nanolayered structures to drilling fluids promotes a substantial improvement in the rheological, viscoelastic, and filtration properties, additionally contributing to cuttings removal, and wellbore stability and strengthening. This also offers a unique opportunity to modulate and improve the thermal and lubrication properties of the fluids, which is highly appealing during drilling operations.

## 1. INTRODUCTION

A drilling fluid (DF) or mud is a liquid or slurry used to lubricate and cool the bit and the drill string, remove the cuttings during a drilling operation, and protect the borehole, among others. In energy and water applications, this type of fluid is used to drill the surface to reach deeper reservoirs where oil, gas, or water might be found. DFs play a crucial role in different applications, and their formulation is a major challenge for the oil, gas, water,

**Received:** April 4, 2022  
**Accepted:** May 19, 2022  
**Published:** June 8, 2022



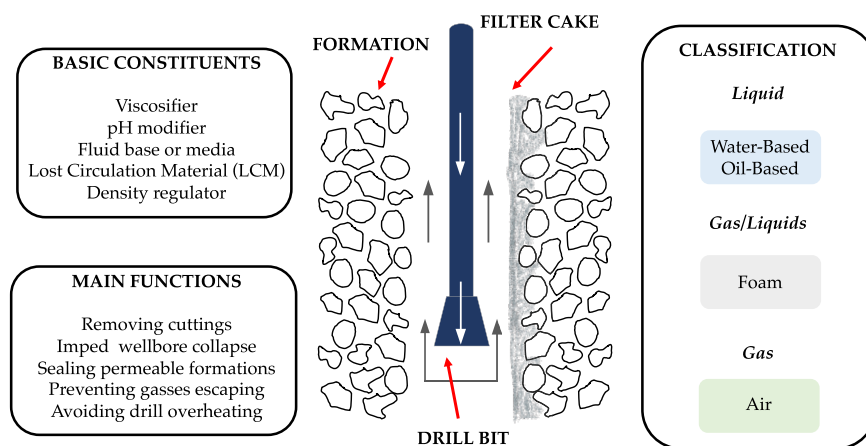


**Figure 1.** Drilling fluids: basic constituents, main functions, and classification.

and infrastructure industries. In some cases, the formulation is pursued to maximize the oil, gas, or water recovery, while minimizing their cost and soil/environmental contamination. The DFs represent about 5–15% of the total costs of the drilling activity.<sup>1</sup> In a similar way, tunnel boring machines efficiency is closely related with the mud characteristics. There is therefore a need for new, improved, environmentally friendly, and cost-efficient drilling fluid formulations that solve the aforementioned issues. DF main functions include the following: (i) controlling the formation pressures (the intrinsic hydrostatic pressure of the DF must always be greater than the natural wellbore hydrostatic pressure to avoid any fluid flux, which can be responsible for the wellbore collapse); (ii) providing adequate buoyancy to transport the cuttings/debris generated during the drilling operation to the surface without a negative environmental impact; (iii) sealing permeable formations encountered while drilling (DFs promote the formation of a thin layer at the surface of the wellbore; this layer is also crucial to avoid fluid exchange with the formation, which often leads to a well collapse); (iv) cooling and lubricating the bit during drilling operations (drilling fluids serve to dissipate the heat generated during drilling operations); and (v) transmitting hydraulic energy to downhole tools.<sup>2–7</sup> Thus, wells require fluids with tailored and improved rheological properties and thermal resistance as well as suitable filtration properties, among others. The final formulation of such fluids must match the wellbore demands, geography, rig capabilities, and environmental concerns. It is also important to mention that modern DF design and maintenance are heavily impacted by the surface and downhole conditions. Most of these fluids must be able to work under extreme conditions, such as under natural or synthetic brines and high-temperature (HT) and/or high-pressure (HP) conditions.<sup>6,8–11</sup> Typical DF formulation would require the following basic constituents: (i) a fluid base or media able to mix with other additives; (ii) a viscosifier, which allows one to control the rheological features of the fluid; (iii) a pH modifier, which allows one to control/avoid corrosion; (iv) a lost circulation material (LCM), which is the main material responsible to control/avoid fluid losses or fluids leaks; and finally, (v) a density regulator, which is responsible for controlling/increasing the hydrostatic pressure.<sup>2,8,10,12,13</sup> These requirements and functions are summarized in Figure 1.

So far, the International Association of Drilling Contractors (IADC) and the American Petroleum Institute (API) have classified DFs in three main categories: (i) water-based drill

fluids, (ii) oil-based drill fluids, and (iii) gas-phased drill fluids.<sup>8–11</sup> According to the literature, more than 90% of the drilling fluids used so far are water-based (WBDF), which means that other formulations based on oil (OBDF) or gas (GBDF) are used in a much smaller percentage.<sup>2,4,8,14</sup> As expected, water-, oil-, or gas-based muds exhibit intrinsic advantages and drawbacks. For instance, OBDFs would offer high temperature and salt/magnesium resistance. They also offer excellent drill bit lubricity, but their main drawback lies in the fact that their formulation is often much more expensive if compared with WBDFs, accompanied by a major negative environmental impact. However, recent research has demonstrated that the environmental impact of such oil-based formulations can be alleviated by using eco-friendly biolubricants derived from vegetable oils.<sup>7,9</sup> Likewise, WBDFs are by far more environmentally friendly. It is relatively easy to modulate their formulation, and their concomitant physicochemical properties, which often leads to very competitive prices if compared with those of OBDFs. In contrast, their main disadvantages lie in the fact that they are much less stable at high temperatures and often exhibit poor lubrication properties if compared with oil-based formulations. Another important issue that WBDFs must overcome is related to the high reactivity to the mineral clays present in the well, which would promote time-dependent borehole problems.<sup>4,8,10,11,15</sup> Modern wells frequently require combination of the aforementioned traits, which is often achieved through the formulation of water-based muds in such a way to reproduce some of the oil-based mud features but with the costs–benefits, biodegradability, and disposal features that water-based muds offer. Relatively few examples of water/oil complex fluids with tailored physical-chemistry properties are currently being formulated by combining esters, poly( $\alpha$ -olefins), glycols, and glycerides, among others. As a matter of fact, standard muds used in water, oil, gas, and tunneling applications will include, but are not limited to, spud muds, bentonite-containing muds, phosphate-containing muds, organic thinned muds (red muds, lignite muds, and lignosulfonate muds), and organic colloid muds.<sup>8,13–16</sup>

All of the aforementioned specificities are considered at present as the major drawbacks in drilling wells operations. In this work, the most recent and relevant findings regarding the development of cost-efficient DF formulations, as well as the trends based on the association of 2D nanoparticles and environmentally friendly precursors, is presented. The advantages and drawbacks of 2D nanostructures such as nanocarbon

allotropes, silicates, and dichalcogenides and their further physicochemical characterization including the rheology and filtration properties are discussed. The main factors affecting the DF performance such as the pH, temperature, ionic strength interaction, and pressure, among others, is also debated. An overview about the fluid flux simulations approaches at the microscale in porous media is also presented, and finally, the future challenges and opportunities linked to developing cost-efficient methods to fabricate tailored nanofluids for DF applications are also listed.

## 2. NANOPARTICLES USED AS ADDITIVES IN DRILLING FLUIDS

Many attempts have been made to modulate the rheological, filtration, and heat transfer properties of DF formulations using nanoparticles as additives, viscosifiers, LCMs, or density regulators by exploiting nanotechnology.<sup>17,18,27,19–26</sup> The enhancement of their properties due to the inclusion of nanomaterials is attributed to their intrinsic properties at the nanoscale. In fact, nanomaterials formulation must ensure that at least one of their constituents possesses sizes up to 100 nm (1 nm = a billionth of a meter).<sup>28–30</sup> At this scale, nanomaterials would exhibit totally different physicochemical properties, including improved electronic properties such as thermal and electrical conductivities, mechanical properties, high specific surface area, magnetism, quantum effects, and antimicrobial activity, among others, if compared with their macroscopic counterpart.<sup>19,21,23,29,31–34</sup> Most of the latter characteristic features are often absent in their macroscopic form, and they are closely related to their sizes and morphologies, which can vary from nanoparticles with well-defined geometry (spheres, triangles, squares, rhombuses, and plates), nanorods, nanotubes, nanosheets, etc.<sup>28,29,35</sup> Nanomaterials are classified as zero-dimensional such as nanoparticles, one-dimensional such as nanorods nanostructures, two-dimensional such as flat layer-like nanoparticles, and three-dimensional such as those nanostructures formed by the interaction of two or several nanoparticles.<sup>28,30,36</sup> Typical nanoparticles used so far in drilling mud formulations include but are not limited to carbonaceous nanostructures (carbon, buckminsterfullerene, carbon nanotubes, and graphene),<sup>37–44</sup> copper oxide (CuO),<sup>45</sup> zinc oxide (ZnO), titanium dioxide (TiO<sub>2</sub>),<sup>46</sup> yttrium oxide (Y<sub>2</sub>O<sub>3</sub>), ferric oxide (Fe<sub>2</sub>O<sub>3</sub>), silicon dioxide (SiO<sub>2</sub>),<sup>47</sup> alumina (Al<sub>2</sub>O<sub>3</sub>), bismuth ferrite,<sup>48</sup> nanocellulose, nanoclays, and molybdenum disulfide (MoS<sub>2</sub>).<sup>19,21,23,24,26,49–53</sup> The fabrication of high-performance hybrid muds based on the association of two or more of the preceding nanoparticles has also been reported.<sup>21,23,24,54–56</sup>

To date, several complex nanofluids aiming to modulate the wellbore and thermal stability, the drill/bit lubrication, and the reactivity with the clay in the shale reducing the hydrates formation within the fluid circulation system have been developed. Gallardo et al. (2018) reported the formulation of WBDFs using silica nanoparticles of 12 nm. They reported that the rheological and filtration properties of such nanofluids were comparable with their oil-based counterparts. They also claimed that the addition of silica NPs to their formulation would have potential applications to minimize shale permeability, fluid leaks, and pore pressure, which would improve the wellbore stability.<sup>47</sup> Similarly, Beg et al. (2020) recently demonstrated that the addition of TiO<sub>2</sub> nanoparticles of 250 nm to water-based mud formulations dramatically improves their thermal stability and rheological properties.<sup>46</sup> In the same way, a very interesting

series of nanofluids was reported by Saffari et al. (2018). They reported the fabrication of tailored drilling muds by using various nanostructured borates-based formulations such as magnesium, zinc, aluminum, and titanium, with variable sizes and morphology (nanoparticles and nanorods). According to their findings, the addition of these nanoadditives increased the extreme pressure performance if compared to the bentonite–water mud counterparts. Besides, they concluded that titanium borate-based additives showed the best tribological properties if compared to the other borates-based formulations.<sup>57</sup> Likewise, Kazemi-Beydokhti and Hajiabadi (2021) very recently demonstrated that the addition of multiwalled carbon nanotube (MWCNT)/poly(ethylene glycol) complex improved the rheological properties (specifically the viscosity and yield stress) of the WBDFs studied. They also claimed that the inclusion of such nanomaterials in their systems improved their carrying capacity (buoyancy) at different temperatures, reduced the fluids losses, and would potentially reduce the risk of formation damage.<sup>58</sup>

Among the various nanomaterials that have been recently used for DF formulations, 2D nanomaterials deserve special attention because of their unique morphological sheet-like structural features. Two-dimensional structures exhibit a huge specific surface area (SSA) and aspect ratio (large lateral length/thickness), with a typical thickness of a few nanometers, while their lateral size could vary from a few dozen nanometers to a few dozen micrometers. They possess particularly remarkable physicochemical and electronic properties (electrons can be confined throughout the plane), with a very high mechanical strength, flexibility, and optical transparency.<sup>53,59–61</sup> Several 2D nanomaterials are currently exploited in different research areas. They include but are not limited to graphene, transition metal dichalcogenides (TMDs) such as MoS<sub>2</sub> and MoSe<sub>2</sub>, hexagonal boron nitride (h-BN) metal organic frameworks (MOFs), covalent organic frameworks (COFs), black phosphorus (BP), natural hydrate clay minerals (i.e., layered vermiculite), silicene, and MXenes.<sup>53,59,61,62</sup> Their potential for use in industrial applications has increased exponentially over the past decade thanks to the development and improvement of innovative and cost-efficient synthesis methods. As far as drilling fluids are concerned, a very interesting work has been recently reported by Hong et al. (2019). They developed a WBDF using MoS<sub>2</sub> flakes as a 2D layered nanomaterial, with a thickness of 1–2 nm and various diameters, ranging from 300 to 650 nm. They claim that these additives promoted a shear-thinning behavior and an increase in viscosity and thermal conductivity. These features are highly appealing to enhance the buoyancy of the formulation, which would facilitate the cuttings' transportation during drilling operations.<sup>49</sup> In the same way, Liu et al. (2017) reported the advantages of preparing WBDF by employing 2D Laponite nanoparticles. Such nanofluids exhibited very good rheological properties with a shear-thinning behavior. The addition of layered 2D Laponite promoted the formation of a filter cake, preventing the water flux penetration into the formation, with a concomitant improved fluid loss. These findings suggest that Laponite-based muds have huge versatility as additives in drilling fluid formulation.<sup>63</sup> Likewise, Zhuang et al. (2017) also studied the formulation of DFs using nanolayered organo-montmorillonite (OMt) and fibrous organo-palygorskite (OPal) nanoparticles as additives. They claimed that the use of such nanostructures would improve the rheological and thermal properties.<sup>64</sup> Similarly, Kosynkin et al. (2012) reported the fabrication of water-based mud with 2D graphene oxide

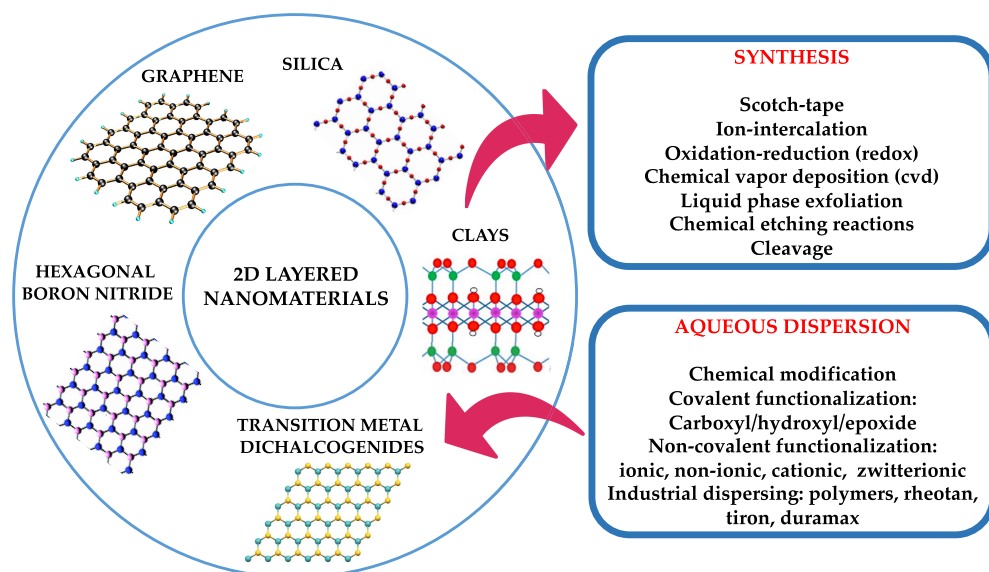


**Figure 2.** Two-dimensional layered nanomaterials used in WBDF formulations and their main synthesis and aqueous dispersion routes.

flakes (GOFs) of two different sizes. They reported that the addition of small quantities of GOFs (as low as 0.2 wt %) promoted a shear-thinning behavior enhancement, higher temperature stability, and reduced fluid losses if compared with their clay-based formulations counterparts.<sup>42</sup> They also claimed that methylating the GOFs increases the stability in saline environments, which would be suitable for brine-based muds formulations.<sup>42</sup>

### 3. FORMULATION AND PHYSICOCHEMICAL CHARACTERIZATION

Since the first attempts by product developers to produce in the early 1910s tailored fluids for drilling operations, the rational designing of innovative, cost-efficient, and eco-friendly WBDFs that meet the industrial requirements remains at the present time by far as one of the most appealing and prolific business interests for companies specialized in developing and commercializing engineered drilling fluids. The tremendous advances in chemistry, fluid mechanics, heat transfer, and nanotechnology, combined with the modern characterization tools and equipment available in the market, are driving a huge improvement in drilling operations efficiency and well productivity.<sup>3,17,37</sup> In this context, any new WBDFs formulation must exhibit a specific functional ability accompanied by distinctive physical and chemical properties specified by the API protocols. Such requirements are gathered in API Recommended Practices (RP) guidelines which offer standard procedures for determining the physical and chemical characteristics of such composite materials. Specifically, drilling fluid formulation must follow the active API specification 13 A (SPEC 13 A, published in 2019), and the WBDFs must fulfill specifically the current and active API-RP 13B1 protocol (5h edition, published in 2019), which provides the minimum set of accepted worldwide physicochemical characteristics and the standard procedures to analyze the aforementioned fluid formulations.<sup>65,66</sup> The latter instruments provide, in a very clear way, the physicochemical features necessary to fulfill the industrial requirements but also the recommended procedure to characterize such fluids. Specifically, these documents offer protocols for determining density; viscosity; gel strength (GS);

filtration; sand, water, and solids contents; pH; salinity; and chemical analyses for calcium and magnesium. These guidelines also provide improved methodologies to determine the shear strength, conductivity, corrosion monitoring, and sag testing, among others, which would be very useful depending on the intended application. For instance, water-based bentonite drilling fluids formulation must exhibit a minimum viscosity of 30 cP at 600 rpm, and maximum filtration loss of 15 cm<sup>3</sup> for a water-based formulation containing 6 wt % bentonite.<sup>65,66</sup>

### 4. FACTORS AFFECTING WBDF FORMULATION USING 2D NANOMATERIALS AS ADDITIVES

The formulation of DFs involves strict requirements ranging from tailored physicochemical needs, environmental constraints, cost–benefits, etc. When developing innovative formulations using 2D nanomaterials, many other important issues arise and thus any scale-up processing must face several potential drawbacks. In this context, factors affecting the DF formulations using 2D nanomaterials as additives will span from the type of nanoparticle, synthesis method, functional groups at the surface, solvation, size, homogeneity, stability, weight content, pH, ionic strength, etc.<sup>3,23,24,37</sup> In the next section, the most important factors affecting the drilling nanofluids performance are detailed.

**4.1. 2D Nanomaterials: Synthesis Methods, Dispersion, and Stability in Aqueous Media.** In order to exploit at industrial scale any mud formulation based on 2D materials, the first requirement would be to engineer readily, cost-efficient, and feasible protocols for the preparation of large quantities of these nanomaterials. Over the past two decades, a lot of attention has been devoted to providing many reliable synthesis methods for the production of 2D layered nanomaterials including but not limited to Scotch tape, cleavage, ion intercalation, oxidation–reduction (redox) reactions, liquid-phase exfoliation, chemical etching, and chemical vapor deposition (CVD), among others.<sup>53,67,68</sup> Most used 2D nanomaterials in drilling fluid applications are derived from layered bulk materials; however, their mass production has severe scalability limitations. Up to date, the most reliable processing techniques suitable for

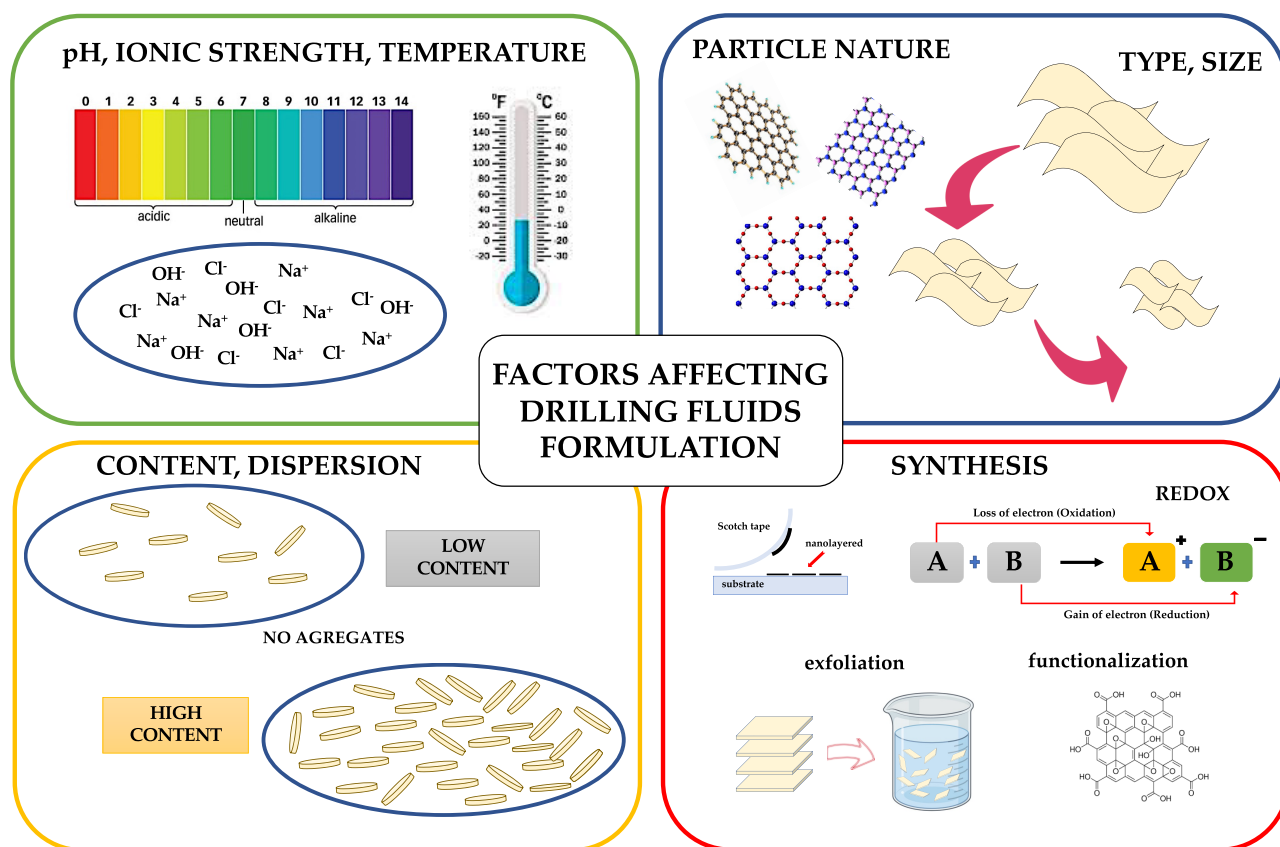


**Figure 3.** Factors affecting WBDF formulations using 2D layered nanomaterials as additives.

industrial application remain by far the aqueous exfoliation and redox reactions.<sup>21,23,37,50</sup>

Figure 2 illustrates some of the main materials, synthesis routes, and dispersion techniques used during the formulation of DFs. Nevertheless, these routes also suffer some shortcomings, such as inherent polydispersity (broad particle diameter and thickness distribution). The latter leads to a heterogeneity in the intrinsic properties of the 2D nanolayered materials that would limit the final performance when included as additives in DF formulation. In the majority of cases, these as-produced 2D layered nanomaterials are still spontaneously agglomerated in liquid media, and it is essential to confer them a hydrophilic character in order to be able to disperse them and exploit them as additives in WBDF formulations even at very low weight content. Besides, the dispersion and stability of these nanofluids will dramatically depend on the nature of the 2D nanostructure but also, on the local environment surrounding the nanoparticle such as the micropolarities present throughout the nanoparticle boundaries.

Few strategies have been proved to be very efficient to stabilize 2D layered nanomaterials in liquid media, including but not limited to chemical modification, surface functionalization with hydrophilic carboxyl/hydroxyl/epoxide functional groups, or use of surface-active agents such as ionic, non-ionic, cationic, and zwitterionic surfactants, aiming at lowering the surface and interfacial tension and stabilizing the interface, or even use of dispersing agents such as polymers, biopolymers, and industrial dispersants such as rheotan, Tiron, Duramax D-3021, Dolapix CE 64, etc.<sup>50,59,69</sup> It is also worth mentioning that, often, subsequent treatments such as separation by ultracentrifugation

are required to reduce the heterogeneity and fully exploit the potential of 2D nanomaterials in large mass applications.<sup>14,70</sup>

**4.2. Nature, Size, and Weight Content Effects.** Several parameters would affect the final performance of the drilling fluid formulation when using 2D nanoparticles as additives, as illustrated in Figure 3. For instance, flakes' size plays an important role in their rheological and filtration properties. For instance, Huang et al. (2021) recently reported the formulation of WBDFs using disk-shaped Laponite nanoparticles with a diameter of about 20 nm and a thickness of about 1 nm. They showed that, upon Laponite content addition, the lubricating property of DF increases. Besides, as the Laponite concentration increases, both the viscosity and the yield point increase accordingly. In contrast, they also showed that as Laponite nanoparticles concentration increases, the fluid losses decrease dramatically. All of these findings were attributed to the nanodisk-like structure and the charged surfaces.<sup>71</sup> Similarly, Ma et al. (2021) recently reported the fabrication of polymer/graphene oxide nanoparticles (PGONs) via aqueous solution polymerization method and investigated their suitability as fluid loss additive drilling applications. They grafted acrylamide molecules on the surface of graphene at two different concentrations. They demonstrated that viscosity and the fluid losses increase as the content of graphene increases. The fluid losses feature was attributed to the fact that addition of PGON promoted a major particle density and thinner and denser filter cake.<sup>72</sup> Similarly, Kosynkin et al. (2012) also showed the effect of the different graphene layer diameter on the fluid losses. In fact, they reported improved filtration properties for a mixture of large flakes graphene oxide nanoparticles (LFGNs) and graphene oxide powder nanoparticles (PGOs) formulation.<sup>42</sup>

In this context, Hajiabadi et al. (2021) also reported interesting rheological and physical properties of WBDF formulations via invert-emulsion method and using three different nanoadditives and weight contents: GO, a native and GO-functionalized Cu-based complex Cu(II) salen. According to their findings, the formulation containing GO/Cu-salen as nanoadditive exhibited a positive effect on the agglomeration of the bentonite platelets. Besides, as the content of GO increased, the formulation showed improved electrical conductivity. These results would suggest that similar formulations would help to reduce formation damage and would be suitable for drilling operations.<sup>73</sup> On the other hand, Alvi et al. (2018) demonstrated similar rheological behavior but using large flakes made of hexagonal boron nitride (h-BN). These fluids behave as non-Newtonian fluids; besides, it was demonstrated that the addition of h-BN promotes a weak increase in the material's viscosity. They also reported that higher viscosity and yield stress occur for the formulation containing 0.1 wt %.<sup>74</sup> A very similar work was reported previously by Wrobel (2017) in which it was demonstrated that formulations with MoS<sub>2</sub> nanoparticles as additives in WBDF systems reduced the average coefficient of friction up to ~30%. They also showed that viscosity scales with the MoS<sub>2</sub> content but with no effect on the filtrate loss performances.<sup>75</sup> All of the aforementioned works evidence how the physicochemical properties and the final performance of drilling fluids formulations would depend on the nature of the 2D nanoparticle, size, and weight content. Moreover, all of these findings also suggest that the predominant effect of these nanoadditives lies in the content. The latter would directly impact on the solution thermodynamics, which predicts stable dispersions upon minimization of the energy required to mix a solute in solvent.<sup>76</sup> It is worth mentioning that better formulations were obtained at very low additive content, which would impact positively any intended industrial use. In fact, the use of nanoparticles in the drilling fluids industry has not been fully exploited due to the cost–benefits repercussions. Thus, future research aiming to improve physicochemical properties, with lower content of additives, accompanied by a readily scalable process to fabricate 2D layered materials would be highly appealing for industrial purposes.

### 4.3. Ionic Strength, pH, Electrolyte, and Temperature

**Effects.** High-performance drilling operations require tailored formulations which often shall work under harsh acidic and alkaline environments. As far as the ionic strength interaction on WBDF is concerned, it is important to mention that the major interactions in water-based formulations are driven by the weakest intermolecular van der Waals forces (electrostatic in nature), such as hydrogen bonding, dispersion forces, and dipole–dipole interactions. In this regard, it is well-established that the pH of any drilling fluid formulation would impact the final fluid performance. As a matter of fact, the most affected rheological properties include the gel strength (GS), yield point (YP), plastic viscosity (PV), filtrate loss (FL), and mud cake thickness (MCT). Besides, it has been reported that bentonitic-based drilling fluids formulation with optimum pH would exhibit not only enhanced rheological and filtration properties but also an enhancement of the rate of penetration which positively impacts the reduction of the pump pressure necessary for the mud circulation. It is important to note that other parameters such as the fluid density remain almost unaltered at different pH ranges. On the basis of actual field data, the majority of the muds used in drilling operations employ DF formulations with most likely neutral to alkaline/basic pH in the range of 8–

12. Thus, an adequate assessment of the pH effect on the rheological and filtration properties of WBDFs formulations using 2D nanolayered materials as additives remains essential for any intended field application. Rassol et al. (2020) reported a systematic investigation on the influence of pH, salinity, and temperature in WBDFs with layered graphene nanoparticulates. They demonstrated that both pH and salinity would impact significantly the formulation rheological properties. They showed that, at basic conditions, the PV and the YP scaled with increasing salinity.<sup>77</sup> In a similar way, Ibrahim et al. (2019) reported the impact of the different intermolecular interactions in WBDFs/graphene formulations. They assessed the influence on the rheological properties of three different formulations using noncovalent functionalized GO by non-ionic, anionic, and cationic surfactants, respectively. According to their findings, the degree of the dispersion of graphene nanolayers would negatively impact the final rheological performance. They also reported that as graphene is better dispersed, the formulation exhibits enhanced shear-thinning properties.<sup>78</sup> In this context, very recently, Ma et al. (2022) reported the assessment of the graphene-functionalized nanoplatelet dispersion at different harsh environments such as pH, high electrolytes content, and high temperature. With this purpose, they used grafted poly(3-sulfopropylmethacrylate potassium) (pSPMA) on graphene oxide platelets (GO-pSPMA). They reported significant flake size changes as pH varied from 7 to 11. The latter was attributed to surface charge shielding promoted by the increasing ionic strength. They also reported that the high negative charge density surrounding graphene flakes confers the adequate electrostatic repulsion to stabilize them in concentrated brine, which is very useful in drilling fluid operations.<sup>79</sup> In a similar approach, Gholami et al. (2021) used silicon nano-glass flakes (SNGFs) with 100 nm diameter and 1 μm of nominal thickness on average to formulate WBDFs. These nanostructures exhibit planar-/platelets-like shape and are made of SiO<sub>2</sub>, which is one of the most used additives in drilling fluids formulations. They evaluated the stability of the suspensions by measuring the ζ-potential as a function of the pH.<sup>80</sup> It is worth noting that ζ-potential is a very important parameter in colloidal systems, and it offers a direct relationship with the colloidal stability. It represents the degree of repulsion between similar and adjacent charged particles. In this way, a high negative charge density would be ideal to provoke sufficient electrostatic repulsion to maintain the dispersion of the nanoparticles. Thus, the SGNFs dispersion exhibited the higher negative ζ-potential for pH 9–10, which falls within the pH range of the most used WBDFs. These nanoadditives were demonstrated to be very promising because they showed enhanced filtration loss and improvement of shale stability (by shale swelling inhibition) with no impact on the rheology.<sup>80</sup> The temperature also plays a crucial role in any WBDFs, including those containing 2D layered nanomaterials as additives. In this sense, an interesting work published recently by Xiong et al. (2019) demonstrated the effect of temperature in the 30 °C < T < 260 °C range on the performance of WBDFs formulations containing 2D layered Laponite nanoparticles with 25 nm of diameter and 1 nm of thickness. They concluded that Laponite additives provide excellent viscosifying and thermal stability (up to 260 °C) to the drilling fluids formulations. In fact, they showed that the addition of 1 wt % Laponite promoted a very low viscosity reduction of 20% with the 220 °C thermal aging, which strongly suggests that similar nanocomposites would be excellent candidates for a ultrahigh-temperature viscosifier of WDFs.<sup>81</sup>

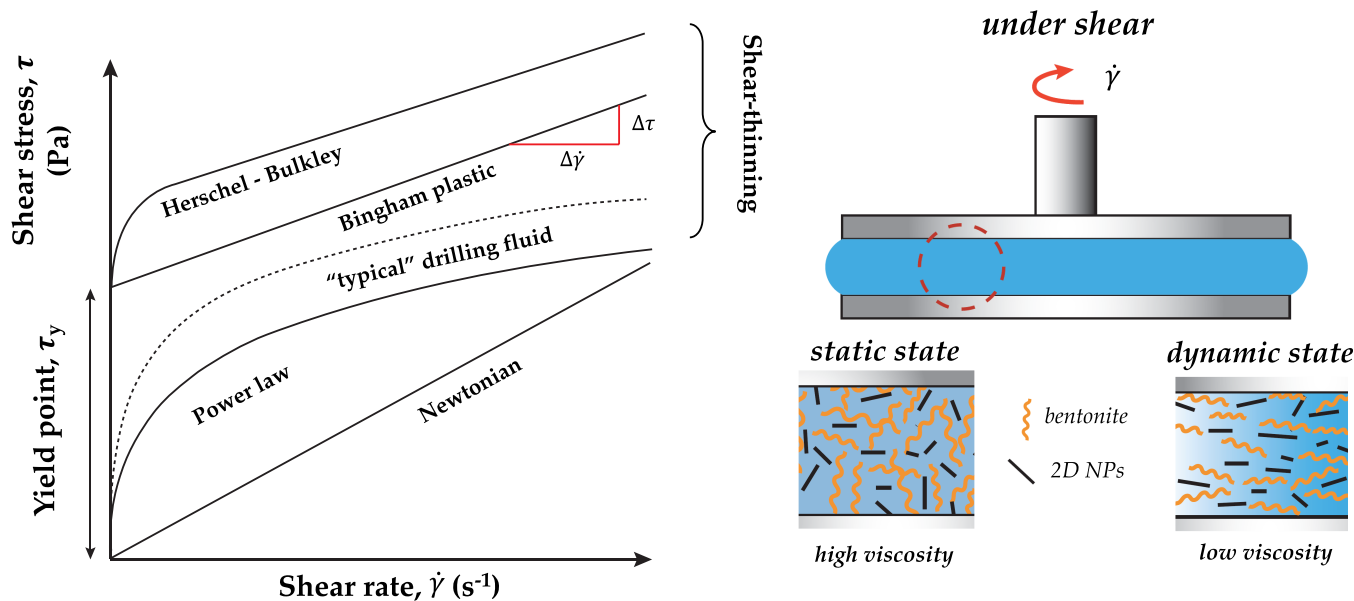


**Figure 4.** Schematic representation of the primary rheology models used in WBDF formulation and the typical behavior of 2D nanoparticles-based formulation under shear (static and dynamic state).

Similarly, Medhi et al. (2021) also showed the temperature response of WBDF formulations containing 2D layered graphene oxide nanoparticles (GONPs) as additives. They reported that the addition of a low content of GONPs (0.5 wt %) to the WBDFs provides excellent thermal stability in the  $0\text{ }^{\circ}\text{C} < T < 100\text{ }^{\circ}\text{C}$  region of temperature, accompanied by an enhancement of their viscoelastic solid properties. In addition, the layered nature of graphene nanoparticles also contributes to improved filtration properties. According to their findings, an enhancement up to 16 times in the viscoelastic modulus was observed, which leads to an improved capacity to transport cuttings during drilling operations.<sup>82</sup>

## 5. RHEOLOGY AND VISCOELASTIC PROPERTIES

The addition of 2D layered nanoparticles will influence dramatically the most important properties of DF formulations such as the rheological and filtration properties. But they also directly/indirectly affect their associated properties such as the lubricating properties, the wellbore stability, the cuttings removal (buoyancy), and wellbore strengthening, among others. Due to the scope of the present work, we will limit our research to provide a recent overview about the different properties affected by the addition of 2D nanolayered materials, focusing on the rheological features and filtration properties, which are crucial to determine the final performance of the DF formulation. For instance, the lubricity or buoyancy are closely linked to the rheological properties of the mud, while the wellbore strengthening is closely related with both the formation of a thin layer “filter cake” at the surface of the formation to impede leaks into/from the formation and their viscoelastic response. The addition of flat 2D layered nanomaterial would improve enormously the fluid losses which directly enhance the wellbore stability.

Rheology has been an important tool in understanding the deformation and flow of matter. One advantage of the research on the stress–strain–time relationship of any material is that it allows one to identify how the material properties are affected by physical parameters such as temperature and pressure. In the context of the DFs, rheology focuses on the fluids-flowing

properties, where the most important physical parameters obtained from rheological measurements are PV, YP, and GS. These properties are very sensitive to the structure, concentration, size, shape, and surface of the nanoparticles added to a DF. In the past, great interest has been paid to the study of similar systems but based on 3D nanoparticles in general.<sup>24,37,83,84</sup> That is why this review is focused on the role of 2D nanoparticles in the rheological properties of water-based systems, in order to provide a fresh look about the latter trends in this field. It is worth mentioning that, as far as our knowledge is concerned, there are only a few works regarding 2D materials and most of them are focused on the use of layered graphene derivatives as additives for DFs.

The rheological analysis of the aforementioned system is thus compulsory in any intended development of innovative DFs. The analysis of PV provides information about the resistivity caused by the solid particulates and the viscosity of the liquid phase. Large PV values imply an increase in the solids content in DF, which means a lower drilling speed.<sup>85</sup> On the other hand, YP and GS refer to the attraction force between particles. YP is also defined as yield stress (YS), which is the minimum shear stress required to initiate flow of a fluid and provides unique information about the capacity to carry drilling cuttings in suspension during the circulation in the wellbore,<sup>86</sup> while GS is related to the capability to solidify.<sup>87</sup> Therefore, GS is associated with the thixotropy of the DFs formulation. According to API 13B-1, the GS is measured using a viscosimeter, first stirring a DF sample at 600 rpm and waiting to reach a steady state, then letting the fluid to stand for a given time (10 s and 10 min), and finally starting the instrument at 3 rpm before recording the reading attained. Although rheological analysis can give the value of these parameters, further comparison with those proposed in the API 13B standard is compulsory.<sup>65,66</sup>

The addition of the nanoadditives in the DFs allows one to control the relationship between the shear stress ( $\tau$ ) and share rate ( $\dot{\gamma}$ ) depending on the intended use. Although some nanofluids containing spherical nanoparticles would exhibit Newtonian behavior, these are not good candidates as DFs because they should exhibit non-Newtonian behavior (shear-

**Table 1. Mathematical Formulation of the Most Common Models Used to Describe the Behavior of WBDFs Incorporating 2D Nanoparticles**

Newtonian	Power Law	Bingham Plastic	Herschel – Bulkley
$\tau = \mu\dot{\gamma}$	$\tau = k\dot{\gamma}^n$	$\tau = \tau_y + \mu_p\dot{\gamma}$	$\tau = \tau_y + k\dot{\gamma}^n$
Viscosity is linearly related to shear rate	This model provides more information at low shear rates.	This model is the most used to describe the rheological properties of drilling fluids. It behaves similarly to the Newtonian model	This combines Power Law model and Bingham-Bulkley model
<b>The variables of the above equations are:</b>			
Symbol	Name	Units	API 13B
$\tau$	Shear stress	Pa - lbf/100ft <sup>2</sup>	
$\dot{\gamma}$	Share rate	s <sup>-1</sup>	
$\mu$	Viscosity	Pa.s - cp	
$\mu_p$	Plastic viscosity	Pa.s - cp	( $\theta_{600} - \theta_{300}$ )
$n$	Dimensionless behavior index	-	( $0 < n < 1$ ) $n = 3.32 \log\left(\frac{\theta_{600}}{\theta_{300}}\right)$
$k$	Consistency index	-	$k = \frac{\theta_{300}}{511^n} = \frac{\theta_{600}}{1022^n} > 0$
$\tau_y$	Yield stress or so-called yield point	Pa - lbf/100ft <sup>2</sup>	<b>Bingham Plastic</b> $\tau_y = \theta_{300} - \mu_p$
			<b>Herschel-Bulkley</b> $\tau_y = \frac{\tau^*{}^2 - \tau_{min}\tau_{max}}{2\tau^* - \tau_{min} - \tau_{max}}$ $\dot{\gamma}^* = \sqrt{\dot{\gamma}_{min}\dot{\gamma}_{max}}$

thinning). It is important to mention that many of these physical parameters can be obtained through a detailed analysis of the rheology curves through analytical fits using common mathematical models. The most frequently used to describe such behavior includes but are not limited to power law, Bingham plastic, and Herschel–Bulkley (see Figure 4 and Table 1). Even though the API standard is based on the Bingham plastic model, the evidence from the literature suggests that not necessarily does this model bring a good correlation with the experimental data for DFs incorporating 2D nanoparticles. The parameters of Herschel–Bulkley are by far more accurate; they have been shown to have correlation coefficients up to 0.99.<sup>84</sup> In the study by Rafieefar et al. (2021) the Herschel–Bulkley model outperformed the other two models in forecasting the rheological parameters of WBDFs using xanthan gum (XG) as a base and low-viscosity carboxymethyl cellulose (CMC-LV) with different concentrations of graphene oxide (GO) as additives.<sup>38,88</sup> Similarly, the Herschel–Bulkley parameters were calculated to evaluate the combined effect of MoS<sub>2</sub>

nanoparticles on 80 °C thermally stable DFs.<sup>89</sup> Likewise, previous studies reported that the Bingham plastic model fits in a very good manner the experimental data of WBDFs using graphene nanoparticles and Laponite 2D layered nanoparticles as additives.<sup>71,90</sup>

All of these models require rheological measurements in steady state, rotation, and oscillation performed in a rheometer.<sup>91</sup> Therefore, steady-state tests accompanied by the adequate fit would offer valuable information on the system viscosity, while the dynamic oscillation tests provide useful information regarding the viscoelastic properties (storage ( $G'$ ) and loss ( $G''$ ) moduli). Both tests should be performed at different conditions (e.g., temperatures, shear rates, and strains) to determine the working range. Furthermore, a time-dependent test is mandatory to evaluate the thixotropic properties of the DFs.

The rheology of 2D layered nanostructures in aqueous phases is not intuitive as they would exhibit very different features depending on several factors. The majority of research



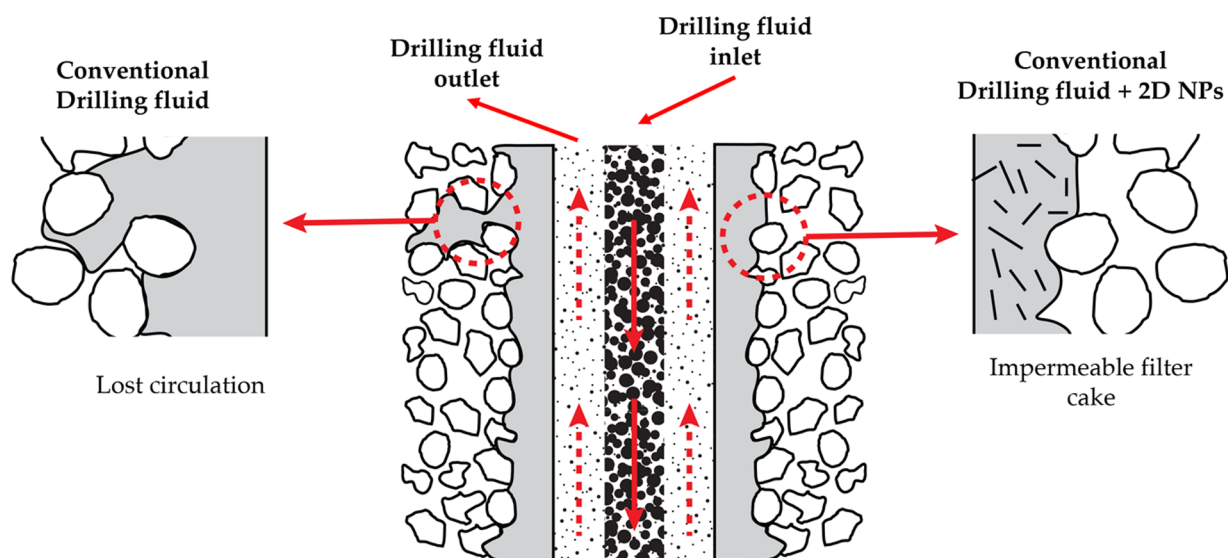


**Figure 5.** Schematic illustration of filter loss of conventional drilling fluid based on bentonite compared to the same drilling fluid but with 2D nanoparticles added.

demonstrates that, under flow, 2D layered nanostructures tend to align parallel to the shear direction.<sup>24,50</sup> However, it has been demonstrated that depending on the content and the flow velocity, different fractions of these 2D nanostructures would align along different directions as in the case of graphene oxide flakes subjected to a different shear stress.<sup>24,50,92,93</sup> In addition to the latter flow-induced alignment, it has been demonstrated that such nanostructures under flow would change from crumpled particles to flattened ones, and more importantly, the spacing between graphene flakes also decreases significantly due to the shear forces. The former phenomena would alter the expected properties of such formulations. Other systems exhibit similar features such as composites made of stiff platelets, disk-like micelles, and crumpled nanostructures.<sup>56,92,93</sup>

Bentonite stands as the most conventional base used in almost all commercially available DFs formulations.<sup>94</sup> In addition to controlling the viscosity, it reduces the fluid losses.<sup>95</sup> Bentonite also tends to form a thixotropic gel in the presence of water.<sup>96</sup> However, this feature deteriorates the properties of the mud cake formed by bentonite, which often impedes removal from the wells.<sup>97,98</sup> It is worth mentioning that this disadvantage also pushed the formulation of alternative nanomaterial-based drilling fluids. As illustrated in Figure 5, the addition of 2D nanoparticles would enhance the rheological properties such as the shear-thinning behavior. As previously mentioned, among the most used 2D layered nanomaterials additives for drilling fluids, graphene nanosheets (GNSs) deserve special attention. Graphene is considered as the simplest carbon structure, which could confer amazing properties to the DFs formulation.<sup>99</sup> A variety of recent works have been published in this area. For instance, Rafieefar et al. (2021) very recently reported that graphene oxide flakes (GOFs) enhanced the shear-thinning behavior by adding solely a tiny amount of GOFs to the formulation.<sup>38</sup> They also demonstrated the significant impact on the shear stress induced by adding 0.15 wt % GOFs to the WBDFs using 0.15 wt % XG and 0.15 wt % CMC-LV. In addition to the modulation of the shear stress, it was also reported that PV increased from 6 to 13 cP, accompanied by a fluid loss of about 18 mL/h, while the recommended value by the API is about 30 mL/h. Similar results were reported by

Medhi et al. and Kosynkin et al., where the addition of GOFs to the WBDFs improved the thermal stability of the system.<sup>42,82</sup> Perumalsamy et al. (2021) also demonstrated that the use of graphene flakes as additives in WBDFs significantly improves PV and YP.<sup>90</sup>

On the other hand, Maiti et al. (2021) studied a DF using boron nitride (BN) layered nanomaterial for deepwater applications.<sup>100</sup> Under offshore conditions the DFs properties change remarkably compared with the aforementioned studies. In such conditions, fluids are subjected to extreme environments, i.e., low temperature and high pressure. They must also overcome the lost circulation which stands as one of the most troublesome problems.<sup>101</sup> These drawbacks might occur when the pumped mud flows into the formations instead of returning up by the wellbore, as illustrated in Figure 5. Therefore, lost circulation is an unwanted effect even for onshore operations. In this context, Razi et al. (2013) reported the rheological properties and fluid losses between conventional DFs (made of 4 wt % bentonite + 3.5 wt % NaCl + 6 wt % CaCO<sub>3</sub> and 0.7 wt % PVP K-90) and DFs with the addition of BN layered nanomaterials (DFs + 2DBN). According to their findings, rheological tests of DFs containing BN showed a significant reduction in PV and YP. Even though the addition of BN decreases the viscosity, further addition enhances the viscosity due to the presence of different types of intermolecular interactions. They also reported that fluid loss decreased from about 17 to 6 mL, and the gel strength decreased by adding 0.6 wt % BN.<sup>101</sup>

It is well-established from a variety of studies that DFs with good shear-thinning properties are widely desired because it is easier to pump them and the wellbore stability and production is also better. The latter would impact positively the drilling costs. With the outstanding features of 2D nanoparticles, they may be a better component for tuning fluid flow behavior. However, more studies are needed to better understand the usage of such nanolayered materials in DFs formulation, either for onshore (high-temperature–high-pressure) or offshore operations (low-temperature–high-pressure).

**Table 2. Rheological and Filtration Properties of Recently Studied DFs Prepared by Incorporating 2D Nanoparticles (See References 38, 49, 63, 71, 73, 74, 89, 90, 105, and 106,<sup>a</sup>**

Nanomaterial used	Characteristics	Experimental details	Performance characteristics		Conclusions and reference
Graphene oxide (GO), xanthan gum (XG), low viscosity carboxymethyl cellulose (CMC-LV) 0.0-3.0 wt.%	GO nanoplatelets: prepared using a modified Hummers approach XG: ~2 Mg/mol	WBDF, formulations tested: GO: 0, 0.05, 0.1, 0.15 wt.% XG: 0, 0.15, 0.3 wt.% CMC-LV: 0, 0.15, 0.3 wt.% Shear rate: 4-1022 rad/s Bentonite was not used in the formulation Herschel-Bulkley model represented the best fit for the rheological data obtained	Viscosity	0.15 wt.% of XG/CMC: Increasing the concentration of GO improves shear thinning 0.15 wt.% and 0.1 wt.% GO: adding XG also improves shear thinning and increases viscosity.	GO and XG improved the rheological characteristics of the fluids evaluated. Adding GO allowed the cake formation and dramatically decreased the fluid loss. Adding CMC had a smaller influence on the rheological characteristics of the DF, compared to XG and GO; however, CMC played a vital role on reducing the fluid loss. 38 Rafieefar et al. (2021)
			Shear stress	0.15 wt.% of XG/CMC: Increasing the concentration of GO increases shear stress 0.15 wt.% and 0.1 wt.% GO: adding XG increases shear stress.	
			PV	0.15 wt.% of XG/CMC: Adding GO increases the PV. Just 0.05 wt.% GO results in an increase from 6 to 11 cp.	
			YP	0.15 wt.% of XG/CMC: Adding GO increases the YP. Just 0.05 wt.% GO results in an increase from 14 to 23 lb/100 ft <sup>2</sup> .	
GO nanosheets (GO-NS), graphene oxide-polyacrylamide (GO-PAM) nanocomposite Evaluation of the controlling filtration properties, particularly in a salty medium 1, 2, 3 g GO 1, 2, 4 g GO-PAM 0.4, 1 g PAM	Bentonite, GO-NS, AM (Sigma-Aldrich) GO: average size of 5 μm GO-PAM prepared via solution polymerization, average size of 20 μm	WBDF, bentonite-based: 500 cm <sup>3</sup> of distilled water, 50 g of bentonite, 5 g of CaCl <sub>2</sub> . Formulations with 20 g of bentonite, 2.5, 5, 10 g of CaCl <sub>2</sub> were also prepared Herschel-Bulkley model represented the best fit for the rheological data obtained for the fluids incorporating bentonite. Data for fluids containing salt fitted the power-law model.	Viscosity and yield stress	Increasing the concentration of bentonite, and decreasing the salt concentration, increases the viscosity and yield stress.	Adding the GO-PAM, at concentrations below 1 wt.%, improves the rheological properties more than the GO-NS. Under static conditions, GO-NS reduced the rate of filtration more than the 104 Movahedi et al. (2021)
			AV and YP	GO-PAM has better performance than GO-NS to improve the properties of high salinity DFs.	
Graphene (Gr) NPs and ester (PC 60) 1, 2, 3 vol.% 30, 60, 90 °C Hot rolling at 65.5°C for 16 h	Ester: PC 60 from Total ACS, which is a product of reaction of glycerol and a tall oil fatty acid blend	WBDF, base mud weight: 9.4 ppg, 283 g of deionized water, 0.5 g of NaCO <sub>3</sub> , 0.5 g of NaOH, 35 g of NaCl, 5 g of modified starch, 1 XC polymer, 25 g of CaCO <sub>3</sub> Viscosity: 21.95 cP; after hot rolling at 65.5 °C for 16 h, decreases to 16.75 cP at 30°C, 1000 1/s Fitting to the Bingham model at 60 °C PV: 8.70 cP, YP: 9.68 lb/100 ft <sup>2</sup>	PV at 60 °C	3 vol.% PC 60: 8.20 cP 3 vol.% PC 60 hot rolled: 9.80 cP 3 vol.% Gr: 7.00 cP 3 vol.% Gr hot rolled: 5.30 cP	Coefficient of friction increases as the plastic viscosity and yield point for ester-based fluids. The addition of PC 60 exhibits higher foaming tendency than the graphene-based fluids 90 Perumalsamy, et al. (2021)
			YP at °C	3 vol.% PC 60: 13.80 lb/100 ft <sup>2</sup> 3 vol.% PC 60 hot rolled: 9.48 lb/100 ft <sup>2</sup> 3 vol.% Gr: 8.80 lb/100 ft <sup>2</sup> 3 vol.% Gr hot rolled: 4.40 lb/100 ft <sup>2</sup>	
			COF	3 vol.% PC 60: 0.087 3 vol.% PC 60 hot rolled: 0.13 3 vol.% Gr: 0.157 3 vol.% Gr hot rolled: 0.253	
GO Cu(II) Salen Cu(II) Salen@GO 0.03 – 0.06 wt.%	Salen is a [O,N,N,O] tetradentate bis-Schiff base ligand	Base invert-emulsion DF: 2:1 diesel oil to water, Glucocon 650 EC and Tween 80 emulsifiers, 22.5 g of Na bentonite, 4 g of NaOH, 500 mg of NP, pH 8.5 PV: 0.037 Pas at 25°C EC: approx. 2.3 mS Yield stress: 5.135 Pa at 25°C Early tertiary Sachun formation, southern Iran	PV 25°C, 0.06 wt.%	GO: 0.017 Pas Cu(II) Salen: 0.017 Pas Cu(II) Salen@GO: 0.020 Pas	GO reduces the electrical conductivity of the base DF, which is not adequate for electrical well logging. The DFs show shear-thinning behavior. 73 Hajjabadi, et al. (2021)
			Yield stress, 25°C, 0.06 wt.%	GO: 0.208 Pa Cu(II) Salen: 0.019 Pa Cu(II) Salen@GO: 0.426 Pa	
GO 0.1-0.5 wt. %	3-7 plies, thickness of 2-7 nm, 0.08 g/cm <sup>3</sup> apparent density, 0.12 g/cm <sup>3</sup> tap density	WBDF, base mud weight: 10 ppg, 303 cm <sup>3</sup> of distilled water, 0.25 g of soda ash, 5 g of polyanionic cellulose, 1 g of Xanthan gum, 7 wt. % of amine, 60 g of barite PV: 17 cP, 10 ppg; AV: 28 cP; YP: 20 lb/100 ft <sup>2</sup> ; GS: 6 and 8 lb/100 ft <sup>2</sup> at 10 s and 10 min Follows the Herschel Buckley non-Newtonian model	PV	GO: 19-21 cP, 9.65 ppg PB: 20-25 cP, 9.68 ppg	Addition of NP does not affect significantly the base mud weight, but improves the rheological properties. PV, YP, GS are increased, filtrate control and the swelling of the formation are improved 105 Lalji, et al. (2021)
			AV	GO: 17 cP PB: 17-26 cP	
			YP at 0.5 wt.% GO	GO: max. 31 lb/100 ft <sup>2</sup> PB: max. 55 lb/100 ft <sup>2</sup>	
Pure-bore (PB) 0.1-0.5 wt. % (micron size)	5-200 μm, 0.3-0.8 g/cm <sup>3</sup> bulk density	Murree shale formation, northern Pakistan: 63% of silicates, 13.6% smectite, 6.7% kaolinite, 5.7% illite, 6% carbonates, 5% iron ores	GS	GO: max. 8 lb/100 ft <sup>2</sup> at 10 s and 0.5 wt.%; min. 6 lb/100 ft <sup>2</sup> at 10 min and 0.2 wt.% PB: approx. 15 and 17 lb/100 ft <sup>2</sup> at 10 s and 10 min, at 0.5 wt.%	
			FL	GO: almost 5 mL at 0.5 wt.% PB: almost 15 mL of 0.5 wt.%	

Table 2. continued

Nanomaterial used	Characteristics	Experimental details	Performance characteristics		Conclusions and reference
MoS <sub>2</sub> nanosheets, 1-2 nm thick MoS <sub>2</sub> multilayers, 5-10 nm thick 1, 3 and 5 wt.%	Nanosheets-small (N-S): 100-400 nm Nanosheets-big (N-B): 300-600 nm Multilayers-small (M-S): 100-400 nm	Base fluid: deionized water, 5 wt.% of bentonite Thermal conductivity: approximately 0.58 W/m·K	1 wt.% MoS <sub>2</sub> : Viscosity and shear stress increased, except for N-S 3 wt.% MoS <sub>2</sub> : M-S fluid showed the higher shear stress and viscosity 5 wt.% MoS <sub>2</sub> : N-B fluid showed the higher shear stress and viscosity		MoS <sub>2</sub> NP strongly strengthened shear thinning, DF shear stress and viscosity increased linearly with increased MoS <sub>2</sub> NP concentration
	Multilayers-big (M-B): 400-650 nm		Shear thinning effect of MoS <sub>2</sub> attributed to 2-D structure and the low coefficient of friction The NP added increase the thermal conductivity in this order: N-B, M-S, M-B, N-S		<sup>49</sup> Hong, et al. (2019)
MoS <sub>2</sub> NPs 0.09, 0.19, 0.26, 22, 50 and 80 °C	MoS <sub>2</sub> NP in a 30 wt.% water solution from US Research Nanomaterials. Density 4.8 g/cm <sup>3</sup> , coefficient of friction 0.03-0.05, Mohs hardness 1-1.5.	WBDF, base fluid: 350 g of water, 10 g of bentonite, 0.6 g of DUO-VIS biopolymer, 3.2 g of anhydrous soda ash, 150 g of barite, 0.9 g lignosulfonates, 6 drops antifoaming agent  Herschel Bulkley and Bingham models used	PV	Base DF: 11 cP (20°C), 7.5 cP (80°C) 0.26 wt.% MoS <sub>2</sub> : 12.5 cP (20°C), 6 cP (80°C)	At room T and P 0.26 wt.% of MoS <sub>2</sub> improve lubricity (weak interlayer forces), thermal and electrical conductivities. The base and MoS <sub>2</sub> modified DFs are thermally stable up to 80 °C. The PVs decrease as the T increase. The addition of MoS <sub>2</sub> did not show significant impact on viscoelasticity. There is no significant variation of the AV.  <sup>89</sup> Belayneh et al. (2021)
			YP	Base DF: 12.5 lb/100 ft <sup>2</sup> (20°C), 13 lb/100 ft <sup>2</sup> (80°C) 0.26 wt.% MoS <sub>2</sub> : 14 lb/100 ft <sup>2</sup> (20°C), 15 lb/100 ft <sup>2</sup> (80°C)	
			COF	Base DF: approx. 0.24 0.26 wt.% MoS <sub>2</sub> : decreased 27%	
			Thermal conduct.	Base DF: approx. 0.605 W/mK 0.26 wt.% MoS <sub>2</sub> : increased 7.2%	
			Electrical conduct.	Base DF: approx. 7.8 mS/cm 0.26 wt.% MoS <sub>2</sub> : increased 8.8%	
			FL	Base DF: 5.2 mL 0.26 wt.% MoS <sub>2</sub> : 5.4 mL MoS <sub>2</sub> and lignosulfonate may have caused poor internal structure of the mud cake	
Laponite (LAP, synthetic hectorite or smectite clay, diameter ~20 nm, thickness ~1 nm) 0, 0.5, 1, 1.5, 2 wt.%	Laponite 1 wt.% of laponite suspension: 20.62 nm average size, 0.7-1.3 g/cm <sup>3</sup> , 300-400 m <sup>2</sup> /g BET	WBDF, base fluid: 400 mL of deionized water, 16 g of bentonite  Outcrop shale from Guanghan city, China (41% quartz, 15% calcite, 4% k feldspar, 12% anorthose, 10% illite, 12.5 ratio illite to smectite) BJH analyses: 7.838 m <sup>2</sup> /g surface area, 0.020 cm <sup>3</sup> /g pore volume, 3.824 nm average pore size	Plugging perform.	Water-treated shale: 14.984 m <sup>2</sup> /g BJH surface area 2 wt.% Laponite-treated shale: 10.791 m <sup>2</sup> /g BJH surface area	The disk-like nanostructure and surface charges of Laponite result in better shale inhibition potential than the
		PV	Base fluid: ~3.4 mPa·s 2 wt.% LAP: ~6 mPa·s		
	surface area, pH 9.8 at 2 wt.% aqueous suspension		AV	Base fluid: ~5.5 mPa·s 2 wt.% LAP: ~33 mPa·s	commonly used KCl and polyamine. Laponite DFs exhibit good plugging performance and could reduce formation damage. It also increases lubricating properties and can reduce fluid loss volume.  <sup>71</sup> Huang et al. (2021)
			YP	Base fluid: ~1.3 Pa 2 wt.% LAP: ~27 Pa	
			GS	Base fluid: ~1 Pa at 10 s, ~3.5 Pa at 10 min 2 wt.% LAP: ~30 Pa at 10 s, ~47 Pa at 10 min	
			FL	Base fluid: 22.8 mL 2 wt.% LAP: 13.2 mL	
			COF	0.25 wt.% LAP: ~11% reduction 2 wt.% LAP: ~32.3% reduction	
Laponite 1, 2 wt.% Bentonite 4 wt.% Shear rate: 0.1-1000 rad/s	Laponite RD (Redwood Company, UK) Diameter smaller than 50 nm.  Sodium bentonite (Sigma-Aldrich, USA)	WBDF, base fluid: 0.5 wt.% poly-anomicrocellulose (PAC)  Weighted DFs: WBD-L: 300 g of water, 3 g of Laponite, 1.5 g of PAC, 180 g of barite, density is 1.4 g/cm <sup>3</sup>  WBD-B: 300 g of water, 12 g of bentonite, 1.5 g of PAC, 180 g of barite, density is 1.4 g/cm <sup>3</sup>	AV at 1000 rad/s	1 wt.% LAP/0.5 wt.% PAC: 28.2 mPa·s 4 wt.% bentonite/0.5 wt.% PAC: 32.2 mPa·s	1 wt.% Laponite was better at improving the shear-thinning behavior compared to 4 wt.% bentonite. The WBD-L showed a higher gel strength and temperature resistance than WBD-B.  <sup>63</sup> Liu et al. (2017)
			YP	1 wt.% LAP/0.5 wt.% PAC: 5.19 Pa 2 wt.% LAP/0.5 wt.% PAC: 24.82 Pa 4 wt.% bentonite/0.5 wt.% PAC: 3.13 Pa	
			Oscillat. freq. sweep test	1 wt.% LAP/0.5 wt.% PAC had higher G' than 4 wt.% bentonite/0.5 wt.% PAC	
Boron nitride (BN) particles 0.06 - 0.4 wt.%	BN: 250 nm average length, and with nanometric lateral dimensions, density of 2.29 g/cm <sup>3</sup> , Mohs hardness of 2	WBDF, base fluid: 500 g of water, 0.5 g of carboxymethyl cellulose polymer, 2.5 g of KCl, 25 g of bentonite Yield stress: ~1.21 Pa; pH 8.89; filtrate loss: 14 mL; COF of 0.42	Yield stress	0.2 wt. % BN: ~1.80 Pa 0.4 wt. % BN: ~1.41 Pa	Adding 0.0095 wt.% of BN or Fe <sub>2</sub> O <sub>3</sub> NP reduced the COF. Fe <sub>2</sub> O <sub>3</sub> NP reduced API static filtrate loss by 14%; adding BN did not affect the filter loss. Data fitted the Herschel-Bulkley fluid model.  <sup>74</sup> Alvi et al. (2018)
			FL	0.2 wt. % BN: 15 mL 0.4 wt. % BN: 15 mL	
			COF	0.2 wt. % BN: 0.29 0.4 wt. % BN: 0.33	
Fe <sub>2</sub> O <sub>3</sub> NP 0.06 - 0.4 wt.%	Fe <sub>2</sub> O <sub>3</sub> NP: size smaller than 50 nm.	WBDF, base fluid: 500 g of water, 0.5 g of Xanthan biopolymer, 2.5 g of KCl, 25 g of bentonite Yield stress: ~3.5 Pa; pH 8.89; filtrate loss: 14 mL; COF of 0.3	Yield stress	0.2 wt. % Fe <sub>2</sub> O <sub>3</sub> : ~6.8 Pa 0.4 wt. % Fe <sub>2</sub> O <sub>3</sub> : ~9.3 Pa	
			FL	0.2 wt. % Fe <sub>2</sub> O <sub>3</sub> : 17.8 mL 0.4 wt. % Fe <sub>2</sub> O <sub>3</sub> : 15.5 mL	
			COF	0.2 wt. % BN: 0.148 0.4 wt. % BN: 0.147	

<sup>49</sup>Temperature, T; pressure, P; plastic viscosity, PV; apparent viscosity, AV; yield point, YP; gel strength, GS; filtrate loss, FL; coefficient of friction, COF; electrical conductivity, EC.

## 6. FILTRATION PROPERTIES (FLUID LOSSES)

Beyond the importance of the rheological properties in any drilling mud formulations, the filtration also stands as one of the

most important and key parameters to be assessed. It is particularly important for drilling operations through permeable formations, in which the hydrostatic pressure exceeds the formation pressure. Under these conditions, DFs invade the

formation, and this phenomenon is also known as spurt loss. Thus, it is of paramount importance for any DF to quickly form a thin filter cake to bridge the formation's pores which minimizes fluid losses. Right after the formation of this thin layer cake, the flow rate of fluid into the formation is driven by the permeability of the cake layer. In the literature and industry, two types of fluid loss measurements are well-defined, the static/dynamic fluid loss, which stands for the measurements of flow rate into the formation when the DF is not/is being circulated. Typically, the standard static API fluid loss test is carried out in a laboratory/industry at room temperature, during 30 min, at 100 psi by using a Whatman filter paper No. 50. However, the latter protocol often underestimates the realistic fluid loss in a given formation.<sup>8,10,11</sup> To date, either in laboratory or field testing conditions, any filtration experiments carried out on WBDFs must be conducted in accordance with the permeability plugging test (PPT) API 13B-1, which substitutes the filter paper by a 1/4 in. thick ceramic disk with a well-known porosity/permeability.<sup>66</sup> Similarly, for dynamic filtration testing, any filtration experiments carried out on WBDFs must be conducted in accordance with the Fann 90 test, which uses a core made of a ceramic and simulates the shearing produced on the filter cake by the fluid in the annulus.<sup>7</sup> The permeability is affected strongly by particle size and shape. In this context, the use of 2D flat-like nanomaterials would positively impact spurt loss, as a consequence of their ability to pack tightly under static or dynamic flow conditions.<sup>17,21,24,50</sup> The stability of the formulation would also impact the filter cake formation. Indeed, particle aggregation would promote a loose and open network, which would cause an important increase in the rate of filtration (ROF). In a like manner, Aramendiz et al. (2019) reported the formulation and characterization of WBDFs using 2D layered graphene nanoparticles as additives. They assessed the impact of the addition of graphene nanoplatelets (GNPs) to the formulation on both low-temperature/low-pressure (LTLP) and high-temperature/high-pressure (HTHP) API filtration tests. All of the LTLPs tests reported were carried out at room temperature, at 100 psi, and with use of filter paper with 2.7  $\mu\text{m}$  pore size. On the other hand, the HTHP filtration tests were carried out at 120 °C, at 500 psi, and with use of an OFITE filter press. They reported a reduction up to 15/25% in the LTLP/HTHP filtrate, respectively, for a very low graphene content of 0.25 wt %. Beyond the filtration advantages offered by the GNPs inclusion in the formulation, a significant 10% reduction in the filter cake thickness was systematically observed.<sup>102</sup> Likewise, Wang et al. (2018) reported the use of layered magnesium aluminum silicate nanoparticles (MASNPs) of 50 nm diameter as additives in WBDFs. Despite that this formulation would not substantially improve the filtration properties, they produced much smoother filtrate cakes which were able to plug the nanopores. The latter property is therefore in high demand for WBDFs used in drilling operations.<sup>103</sup> A similar work was recently published by Huang et al. (2019) in which they use nanolayered Laponite to fabricate tailored WBDFs. In spite of such a formulation not showing significant influence on fluid loss, they assessed the temperature effect. They demonstrated that fluid loss was almost unaltered in the temperature range of room temperature (RT) <  $T$  < 180 °C. All of these facts are in total concordance with other works, which reported that Laponite nanoparticles exhibited excellent properties by inhibiting clay swelling and maintaining wellbore stability.<sup>104</sup> All of these works demonstrate that filtration property, which is one of the most important in drilling fluids formulation, can be

significantly improved upon addition of 2D layered nanomaterials. All of these flat-like nanomaterials demonstrated low fluid loss volume, which is critical to reducing fluid invasion into the formation. The latter is the main cause of wellbore instability and collapse. Beyond the afore cited properties, the industrial scale-up feasibility of such formulation must also overcome the environmental and the cost–benefit impacts. However, most of the aforementioned 2D layered nanomaterials are abundant in nature and eco-friendly. Finally, in spite of the fact that the current cost of producing large quantities of WBDFs using 2D layers remains relatively high if compared with their counterpart NP-free bentonitic muds, the use of such additives often requires lower quantities of these 2D layered nanomaterials to reach better performances than commercial WBDFs. Table 2 summarizes some aspects of the performance of WBDF prepared by incorporating different types of 2D nanomaterials. This performance encompasses the rheological and filtration properties of the DFs.

## 7. SIMULATION OF FLUIDS IN POROUS MEDIA AT THE MICROSCALE

A big concern regarding the DF performance and its potential use in field operations is related to the formation collapse during drilling operations. The latter will be enhanced due to leaks from/to the wellbore due to the presence of DFs flowing within the well. Thus, any analog and numerical simulation methods allowing one to evaluate fluid flows in porous media at the micro-/macroscale would be valuable for the assessment of DF suitability and could dramatically reduce the drilling operations cost. In this section, the physical problem of the fluid flow through porous structures at the microscale is introduced, from the numerical point of view. The simulation approaches described could provide useful information regarding the potential fluid losses during drilling, which will depend on how fluids flow in the porous structure. The model system involves the use of two nonmiscible phases (i.e., water and oil), but it can be extrapolated to a water-based drilling fluid and oil to assess their potential use in drilling operations. As far as the knowledge of the authors is concerned, not much literature has been reported so far addressing analog and numerical simulation methods, used to research fluid flow in porous media when studying DFs.

Mathematical modeling and simulation of flow in porous media has been an approach of critical interest for practical applications of oil recovery.<sup>107,108</sup> Its comparative low cost and potentially high yield way to generate strategies for oil recovery make it a tool of choice and an integral part of oil and enhanced oil recovery protocols.<sup>109</sup> Modeling and simulations cover a broad spectrum of behaviors from macroscopic displacement of different phases to pore level interactions between oil/displacing fluid and the solid phase and even turbulent flow within pores.<sup>110</sup> There are also different physical variables of interest, such as wettability (fluid rock interactions), interfacial tension (fluid–fluid interface), viscosity (intrinsic property of fluid), permeability (intrinsic property of static solid phase), porosity, multiphase relative permeability (interactions among multiply-flowing phases), tortuosity (characterization of the static solid phase), and fractality. Among others, the tools used to describe them with different computational strategies include sharp and diffuse interface models, multiphase flow solvers, finite element methods, upscaling methods, lattice Boltzmann, dissipative particle dynamics, accelerated flash calculations, and deep learning algorithms.<sup>111–113</sup> This work is focused on macroscopic

flows, well above the pore scale, where the porous medium is seen as an effective medium with averaged permeability properties described by continuum equations. The continuum equations generally used in such a scale of simulation are the continuity equation and the momentum conservation equation. For the case of incompressible flows ( $\nabla \cdot v = 0$ ):

$$\frac{\partial \rho}{\partial t} + \nabla \cdot [\rho v] \quad (1)$$

$$\frac{\partial}{\partial t} [\rho v] + \nabla \cdot [\rho v v] = -\nabla p + \nabla \cdot [\mu [\nabla v + (\nabla v)^T]] + f_b \quad (2)$$

where  $\rho$  is the fluid density,  $v$  is the fluid velocity,  $p$  is the fluid pressure,  $\mu$  is the viscosity, and  $T$  stands for the transpose. Finally,  $f_b$  is the body force applied externally to the fluid. The equations can be simplified for constant viscosity models. In the case of thermodynamics considerations, an energy conservation equation must be considered which considerably increases simulation times,

$$\frac{\partial}{\partial t} [\rho c_p T] + \nabla \cdot [\rho c_p v T] = \nabla \cdot [\kappa \nabla T] + Q \quad (3)$$

where  $T$  is the temperature,  $c_p$  is the specific heat at constant pressure,  $\kappa$  is the thermal conductivity, and  $Q$  is the transferred heat. Additional equations may have to be included if phases are not conserved due to chemical reactions or formation of new phases such as when carbon dioxide is injected.<sup>108</sup> Algorithms that emphasize oil recovery through stable displacement generally neglect the energy conservation equation and focus on the evolution of the interphase. This is known in the literature as the Brinkman equations approach.<sup>114</sup> The latter equations modify the purely hydrodynamic equations above to include features of the matrix in which the flows occur

$$\frac{\partial(\epsilon_p \rho)}{\partial t} + \nabla \cdot [\rho v] = Q_m \quad (4)$$

$$\begin{aligned} \frac{\partial}{\partial t} \left[ \frac{\rho v}{\epsilon_p} \right] + \nabla \cdot \left[ \frac{\rho v v}{\epsilon_p} \right] \\ = -\nabla p + \nabla \cdot \left[ \frac{\mu}{\epsilon_p} [\nabla v + (\nabla v)^T] - \frac{2}{3} \mu (\nabla \cdot v) I \right] \\ - \left( \frac{\mu}{\kappa} + \frac{Q_m}{\epsilon_p^2} \right) + F_i \end{aligned} \quad (5)$$

where  $\mu$  is the dynamic viscosity of the fluid,  $\epsilon_p$  is the porosity,  $\kappa$  is the permeability of the porous medium, and  $Q_m$  is a mass source/sink. External forces are included in the  $F_i$  term. This formulation includes inertial effects and the possibility of changed porosity with time.  $Q_m$  includes the injection of material into or out of the simulation cell. For the inclusion of temperature and pressure effects on the fluids, the previous equations must be coupled with an equation of state, relating density to temperature and pressure. Flow of heat, not within the scope of this review, would also require equations of state to complement the energy flow equation.

**7.1. Analog Simulations.** Also available are analogic simulations of flow in porous media that can appear as a “disappointingly” simple representation of the porous medium, such as Hele–Shaw cells and capillary methods, but offer much insights about the behavior of interfaces at different scales.<sup>108</sup>

Figure 6 illustrates a Hele–Shaw cell, which consists of two plates separated by a distance and width between which there

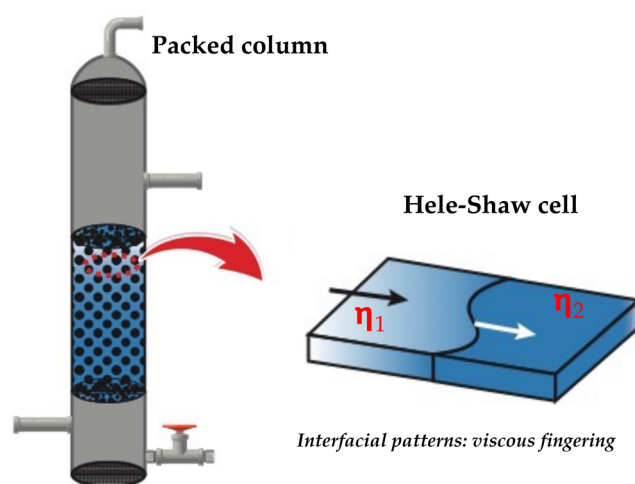


**Figure 6.** Typical Hele–Shaw cell, which is a crude but practical and analyzable analog simulation of an oil reservoir or packed column of porous material.

are 2 or more phases in contact. The industry standard for these analog simulations is the core permeability studies<sup>115</sup> that only render core scale information and little information on the details of the interfacial behavior. Nevertheless, they do furnish “intact” oil and gas reservoir properties.

The analog simulations are extremely useful in capturing basic instabilities of the displacement front that are crucial for enhanced oil recovery strategies.<sup>108</sup> In the Hele–Shaw setup,<sup>116</sup> where there is a basic displacement of a higher viscosity phase by a lower viscosity phase, the fingering phenomenon (illustrated in Figures 7 and 8) signals the interfacial instability in very well

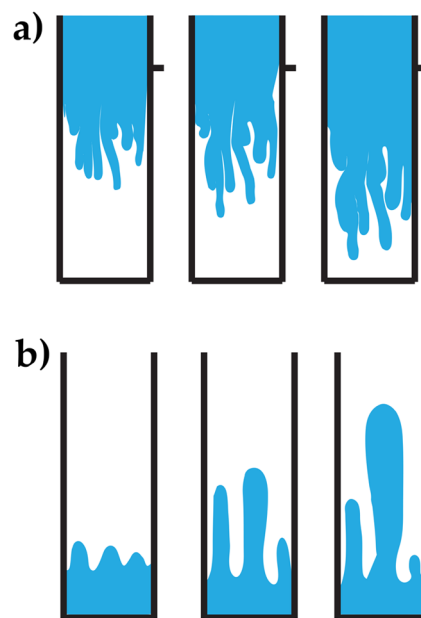


**Figure 7.** (a) Unstable viscous flow fingers under a vertical packed column in the Hele–Shaw geometry. Low viscosity fluid is injected from one end of the cell attempting to displace a more viscous fluid in the cell. (b) Multiple fingers developing on flow velocity of interface.

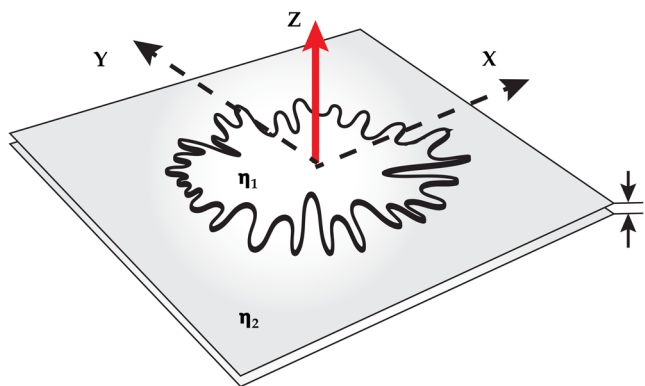


**Figure 8.** Hele–Shaw cell in radial geometry with fingering instabilities.

characterized ways, depending on the flow velocity, width of the cell, and depth of the cell. The latter parameter represents an important feature of the porous medium which is the pore throat width. The model can nevertheless be enriched by including glass beads with various distributions to capture more complicated and larger scale geometries.

A flat interface evolves in the  $x$  direction according to  $x(y) = Ut$ , with  $U$  being the interface velocity and  $y$  the lateral dimension. By introducing a small periodic perturbation in the  $y$  direction of amplitude  $A(t)$ , one gets

$$x(y) = Ut + A(t) \cos(qy) \quad (6)$$

where  $q$  is the wavenumber of the applied perturbation. Considering the depth of cell  $b$  and substituting this perturbation in Darcy's law

$$v(x, y) = -\frac{K_i}{\mu_i} \nabla P(x, y) \quad (7)$$

where  $K_i$  is the permeability of the medium,  $\mu_i$  is the viscosity of the most viscous phase, and  $P(x, y)$  is the pressure across the interface. Following Bensimon et al. (1986), the following behavior for the amplitude is derived:

$$\dot{A} = A \left( \frac{U}{h^2/12\mu} - \gamma q^2 \right) \frac{h^2}{12\mu} q \quad (8)$$

where  $\gamma$  is the surface tension of the interface and  $h$  is the depth of the Hele–Shaw cell.<sup>116</sup> It is clear that if the quantity in the parentheses is positive, the interface amplitude perturbation grows and the evolution is unstable, while if it is negative, it is stable. The sign of the parentheses depends on the velocity of the displacement and the wavenumber of the perturbation. As the

velocity increases, the instability tends to be dominant and more and more wave vector values become unstable.

This is the standard analysis with some more detailed developments related to finger widths in relation to channel widths as precursors of unstable flow.<sup>117</sup> The quest to stabilize the development of instabilities in order to achieve an efficient displacement of oil in the porous matrix by injected fluids is then guided by the interface mechanics. The interface motion is governed by the finger width, the pore size, the interfacial tension, and the viscosity of the high-viscosity phase. There are many ways in which the viscosity contrast can be diminished and the interfacial tension can be manipulated to achieve stability and the Hele–Shaw setup can be a testing ground for different strategies.<sup>108</sup>

The Hele–Shaw setup has been explored further by enclosing glass beads between the plates.<sup>118</sup> This introduces additional scales in the porous space structure and also adds very realistic features such as wetting properties of the displaced and displacing fluids. Flooding with emulsions was proven to enhance high viscous phase recovery, reproducing the observed increased efficiencies in field tests. What could be called a 3D variant of the Hele–Shaw setup that explores the behavior of the pore throats in a porous medium against the flow of emulsions has also been studied.<sup>119</sup> The results show important implications for the evolution of emulsion droplet size as the emulsion moves through the porous medium and the resulting pressure drops at the pore throats. A very interesting recent development of analog simulations such as the Hele–Shaw setup consists of considering a tapered porosity<sup>120</sup> or a tapered width<sup>121</sup> of the Hele–Shaw cell, as observed in Figure 9, which introduced a new element of stability control of the interface. In real life situations, such as those that occur not only in the porous oil-bearing strata but also in systems such as lung airways or printing devices, the porous medium is not uniform and this non-uniformity can be modeled in a Hele–Shaw cell by inclusions either that vary the pore throat width or that change the separation between the Hele–Shaw plates in a particular way. For the case of patterned porous structure within the cell, the new stability criterion reads

$$1 - \lambda + \frac{2\alpha \cos \theta_c}{Ca} \leq 0 \quad (9)$$

where  $\lambda = \mu_1/\mu_2$ , the subscript 2 referring to the invading fluid,  $\alpha$  is the slope of the increasing depth of the cell ( $b(x) = b_0 + \alpha x$ ),  $\theta_c$  is the contact angle to the Hele–Shaw plates to account for wetting effects, and  $Ca = 12\mu_1 U/\gamma$  is the capillary number, where  $U$  is the displacement velocity and  $\gamma$  is the interfacial tension. To make contact with eq 8, higher wavevector terms must be included.<sup>121</sup> This stabilization has been evidenced by Eslami et

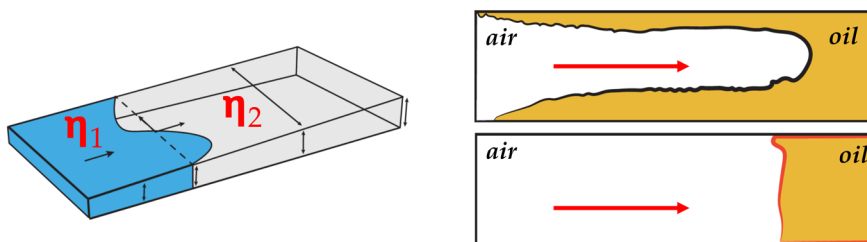


**Figure 9.** Schematization of the compelling stabilization of displacement front produced by a non-uniform depth of the Hele–Shaw cell. The left panel shows the cell geometry; the right panel, the typical fingering in a Hele–Shaw cell with a uniform gap; and the bottom panel, the same flow conditions in a converging Hele–Shaw cell. Adapted in part with permission from ref 121. Copyright 2012 Nature.

al. (2020), where other fingering phases described as rough fingers are also shown.<sup>122</sup>

Another contribution that evidences the stabilization through non-uniformity is the case of structured porous media. The non-uniformity here corresponds to a varying pore radius described by parameter  $\lambda = (r_o - r_i)/l$ , where  $r_o$  and  $r_i$  are the pore radii at the outlet and inlet and  $l$  is the length of the cell. The depth of the Hele–Shaw cell is another dimension that adds three-dimensionality to the system. This is contemplated in the previous models through the wetting angle. Many oil recovery efforts involved changing the salinity of the displacing fluid, and then the interface flow becomes susceptible to electrokinetic effects that can affect the front profile yielding the possibility of electrically enhanced oil recovery.<sup>123</sup> The authors find that in a uniform geometry of the Hele–Shaw cell, fingering phenomena can be controlled by varying the injection ratio of electric current to flow rate. Stability then depends on the relative direction of the flow and current directions.

**7.2. Numerical Simulation Methods.** Numerical simulations of fluid fronts in porous media, in principle, start from the transport, eqs 3, 4, and 5. Equation 3 is the heat transport equation which is generally ignored when *fluid discretization methods* are used, such as those that focus on the Brinkman equations (combination of eqs 4 and 5). Different mesh methods are used to discretize the simulation space depending on the details of the space- and time-dependent dynamics. It is important to distinguish the transport regime in order to address the computational problem with the appropriate equation valid in such a regime. The Darcy law of eq 7 is used to describe a volume large enough to have a well-defined porosity and permeability, which in the statistical sense is known as a self-averaging volume.<sup>124,125</sup> Equation 7 describes fluid motion through a porous medium of permeability and viscosity in the regime of low-velocity flows, for which the pressure gradient is the main driving force. As flow will be dominated by the frictional resistance within the pores, it can also be thought to be valid where the permeability and porosity are small. The derivations in eqs 8–10 are based on this slow-flow regime with more than one phase. One can incorporate non-Darcian effects by including Forcheimer drag terms which are important for higher Reynolds numbers.

To go to higher Reynolds numbers, one must include inertial, density, and velocity effects. For this one must address the problem of flow in porous media with the Brinkman equations (eqs 4 and 5), again in a mesoscopic description where macroparameters are well-defined. The Brinkman equations describe incompressible or compressible flows, where the velocity of flow is less than half the speed of sound in the fluid. As discussed before, the level set method reduces the description of the fluid to the interface, reducing the computational cost, and nothing is said about what happens in the bulk phases. The description then incorporates dissipation by viscous shear. These strategies on the one hand are very efficient numerically, especially for multiphase simulations, for the Level Set method which follows only the interphases benefiting both in accuracy and speed. In Figure 10 is shown a representative snapshot of the behavior of different phases dependent on velocities in simulated unstable two-phase displacement by means of the Level Set method following the interface evolution, simulated with COMSOL software. The criterion for evolving from one to two finger instabilities is given by eq 8.<sup>126</sup>

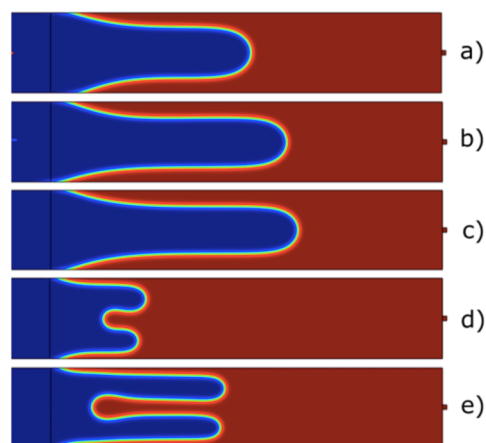


**Figure 10.** Different phases dependent on velocities in simulated unstable two-phase displacement by means of the level set method following the interface evolution, simulated with COMSOL software.

Alternative mesoscopic descriptions that have numerical and speed advantages are the particle-based methods such as *diffusive particle dynamics* (DPD)<sup>127–130</sup> and *smooth particle dynamics*.<sup>131</sup> The latter method is of frequent use in astrophysics adapted to very high velocity flows and even galaxy collisions. The former method, DPD, is more extensively used in flow in porous and fractured media<sup>132</sup> and biological-based applications such as micelles and membranes.<sup>133</sup> Both approaches offer good qualitative agreement with hydrodynamic behavior at the microscale also ignore the energy flow equation, and temperature dependence must be included as supplementary conditions for the behavior of particles. The great advantage of particle-based methods is the adaptation to complex boundary conditions that happen frequently in porous media and also that are mesh-free methods. An interesting work has been reported on the formation of a liquid droplet by SPH simulations. The method captures surface tension effects and density profile of a liquid droplet.<sup>134</sup>

A final set of methods was founded on fluids on a lattice, coming originally from so-called automaton methods and lattices gases.<sup>135</sup> For an automaton one defines a grid of cells which can be “on” or “off” to denote, e.g., the presence or absence of fluid, and the evolution of the fluid presence is defined by rules regarding neighboring occupied and empty cells.<sup>136</sup> It is called an automaton since once an initial configuration is devised, it can evolve by indefinitely propagating or oscillating or stop altogether following the rules. For lattice Boltzmann the set of rules is very simple so they are computationally very fast to implement. The rules follow streaming and collision phases of fluid flow according to the collision time approximation: If there is a lattice where each point has  $m$  neighbors, then  $f_i(r,t)$  is the fluid density at position  $r$  and time  $t$  moving at a velocity  $e_i$  per time step along direction  $i$ .  $f_i(r,t)$  evolves as

$$f_i(r, t + \delta t) = f_i(r, t) + \frac{f_i^{\text{eq}}(r, t) - f_i(r, t)}{\tau} \quad (10)$$

for the collision step, and as

$$f_i(r + e_i, t + \delta t) = f_i(r, t) \quad (11)$$

for the streaming step. It can be shown that starting from these simple rules one can derive the Navier–Stokes equations for

small Reynolds numbers<sup>137</sup> so the method is limited to such a regime, perfectly useful for simulations of fluid flooding in porous media. Very exciting results have been obtained from this simulation tool that holds great advantages: (i) runs efficiently on massively parallel architectures,<sup>138</sup> (ii) can describe multiphase flows with description of droplets and bubbles,<sup>139,140</sup> (iii) adapted to complex geometries within resolution of lattice. The limitations are related to low-Mach/-Reynolds numbers<sup>141</sup> and the translation with regular boundary conditions and parametrization of surface tensions and viscosities and densities in multiphase flow, a problem also with particle-based methods. Another piece of interesting work showed the two-phase flow in a model porous medium by the lattice Boltzmann simulation method for viscosity ratios of  $M = 1/25$  and  $\log Ca = -5$  has been published recently. In this work authors also showed simulation about the differences in wetting and nonwetting fluids.<sup>142</sup>

All of the aforementioned analog and numerical simulation methods stand as the most powerful simulation strategies to evaluate fluids in porous media at the microscale. The physical problem of the pore scale from the numerical point of view has been already largely addressed. Indeed, similar flow simulation scales much larger than the pore microscale has been extensively reported in the literature. As far as DFs formulation is concerned, such simulations would provide useful information regarding the potential fluid losses which will depend on how fluids flow in the porous structure. Future works including not only water, oil, and air phases but also water-based drilling fluid formulation would be necessary and useful to assess their potential use in drilling operations.

## 8. DISCUSSION

Given the technical importance and economic impact that DFs have for a wide variety of industries, they have been extensively researched and developed during the past decades. However, the requirements around their use are constantly becoming more demanding, ranging from those arising from their environmental impact and their associated costs and those issues involving the end users and stakeholders. This has opened several opportunities to incorporate tools such as nanotechnology and simulation to the development of tailored, sustainable, environmentally friendly, and cost-efficient DFs.

Most of the works reported so far are focused on other 1D or 3D nanomaterials, with only a few emphasizing the use of 2D layered nanomaterials. The majority of this related research employing 2D layered nanomaterials is focused on graphene and its derivatives. The use of such nanoparticles in DFs formulations has been limited to replace some of their main components such as the viscosifier, the pH modifier, the LCM, or the density regulators, but, in any case, they are capable of substituting the media/base drilling fluids formulation. It is also worth noting that the base used in the majority of these works makes it difficult to compare the resulting fluids. As a matter of fact, most of the work has been done on model fluids, incorporating materials such as bentonite, barite, and xanthan gum and not using typical DFs formulation which includes the basic constituents and follows API guidelines. The potential of using other types of 2D layered nanomaterials including but not limited to using silicon nano-glass flakes, MoS<sub>2</sub>, disk-shaped Laponite nanoparticles, layered magnesium aluminum silicate nanoparticles, and nanolayered organo-montmorillonite, among others, open even more their potential applications in drilling operations.

It has been demonstrated that the addition of 2D nanostructures as DFs additives promotes a substantial improvement in the rheological, viscoelastic, and filtration properties. But they also offer a unique opportunity to modulate the thermal properties of the fluids, which is highly appealing during drilling operations. Additionally, different 2D nanoparticles have been used as promising additives to ameliorate the filtration properties, reducing thus the fluid losses during wellbore operations. Besides modifying selectively certain DFs properties, the use of 2D nanoparticles also serves to provide lubrication properties improvement (as demonstrated in those works using MoS<sub>2</sub>). Interestingly, the inclusion of 2D nanoparticles (such as those based on silicates) have demonstrated to be good candidates for tailored DF formulations due to its environmentally friendly nature and associated low costs.

The final performance of these formulations using 2D layered nanomaterials would depend on the nanoparticle nature, morphology, shape, size, and concentration; stability; and homogeneity, but also on other factors such as the pH, temperature, ionic strength interaction, salinity, and pressure which affect the final performance of these nanofluids. The control of the rheological properties through the 2D additives would also provide a route to fabricate fluids with customizable yield stress, which is of paramount importance to remove the cuttings from the wellbore. In contrast, not only would the use of 2D hydrous phyllosilicate natural minerals such as nanolayered clays, Laponite, vermiculite, etc., offer the opportunity to reduce the fluid losses but also the presence of these hydrous-based nanoparticles would promote the dissolution of gas in the DFs preventing the formation of crystal hydrates. The chemical mechanisms on how the nanoparticles impede the hydrates formation remains as one of the open debates and needs further investigation.

Finally, the incorporation, due to the aforementioned reasons, of 2D layered nanomaterials would play a crucial role in future commercial applications and developments of sustainable, eco-friendly, and cost-efficient water-based drilling fluids formulations.

## 9. CONCLUSION

In this work, the most recent and relevant findings related to the customization and improvement of water-based drilling nanofluid formulations using 2D layered nanomaterials are presented. The nanomaterials considered include silicon nano-glass flakes, graphene, MoS<sub>2</sub>, disk-shaped Laponite nanoparticles, layered magnesium aluminum silicate nanoparticles, and nanolayered organo-montmorillonite. These nanoparticles have demonstrated their capabilities to replace some of the main DF components such as the viscosifier, the pH modifier, the LCM, or the density regulators. The addition of such nanostructures has been limited so far to 1D or 3D nanoparticles. Solely, a few 2D nanoparticles have been investigated as DF additives, and the majority is focused on graphene-like derivatives. Their incorporation as drilling fluid additives has promoted a substantial improvement in the rheological, viscoelastic, and filtration properties but also their associated lubricating properties, additionally contributing to wellbore stability, cuttings removal, and wellbore strengthening. These improvements are attributed to their flat 2D nature, which is the main characteristic responsible for avoiding mud leaks downhole, even under HT/HP conditions. Besides, their nanosize features also serve to create a filter cake in specific formation's interstitial zones.



Even though DFs have been extensively researched and developed by academia and the private sector, it is worth noting that there is not much literature on commercial drilling fluids, because most of them are subjected to strict regulation and patents. Besides, the full exploitation of the nano-based DFs has been hindered in the past mainly due to the elevated costs associated and multisteps formulations requirements which often hinder their potential application at industrial scale. These illustrate the need of coupling the experimental efforts for improving the performance of DFs with the guide that effective simulation could provide. The simulation approaches at the microscale for fluids in porous media offer the opportunity to run and test different parameters, avoiding expensive and time-consuming laboratory experimentation. Future trends will focus on producing tailored nanofluids with enhanced rheological and filtration properties but also based on eco-friendly additives/precursors and cost-efficient particles.

## AUTHOR INFORMATION

### Corresponding Author

**Camilo Zamora-Ledezma** – *Tissue Regeneration and Repair Group: Orthobiology, Biomaterials and Tissue Engineering, UCAM-Universidad Católica de Murcia, 30107 Murcia, Spain*; [orcid.org/0000-0002-8704-1539](https://orcid.org/0000-0002-8704-1539); Email: [czamora9@ucam.edu](mailto:czamora9@ucam.edu)

### Authors

**Christian Narváz-Muñoz** – *Escola Tècnica Superior d'Enginyers de Camins, Canals i Ports, Universitat Politècnica de Catalunya—Barcelonatech (UPC), 08034 Barcelona, Spain; Centre Internacional de Mètodes Numèrics en Enginyeria (CIMNE), 08034 Barcelona, Spain*

**Víctor H. Guerrero** – *Departamento de Materiales, Escuela Politécnica Nacional, Quito 170525, Ecuador*

**Ernesto Medina** – *Departamento de Física, Colegio de Ciencias e Ingeniería, Universidad San Francisco de Quito, Quito 170901, Ecuador*; [orcid.org/0000-0002-1566-0170](https://orcid.org/0000-0002-1566-0170)

**Luis Meseguer-Olmo** – *Tissue Regeneration and Repair Group: Orthobiology, Biomaterials and Tissue Engineering, UCAM-Universidad Católica de Murcia, 30107 Murcia, Spain*

Complete contact information is available at: <https://pubs.acs.org/10.1021/acsomega.2c02082>

### Funding

This work was financially supported by the “Convocatoria de Ayudas a la Realización de Proyectos de Grupos de Investigación 2020–2021” of the Universidad Católica de Murcia (UCAM), Spain, Reference PMFI-12/21. V.H.G. acknowledges the support of Escuela Politécnica Nacional (EPN)—Ecuador, through Project PIM-20-03. C.N.-M also acknowledges the support of Severo Ochoa scholarship PRE2020-096632.

### Notes

The authors declare no competing financial interest.

## REFERENCES

- (1) Bloys, B.; Davis, N.; Smolen, B.; Bailey, L.; Houwen, O.; Reid, P.; Sherwood, J.; Fraser, L.; Hodder, M. Designing and Managing Drilling Fluid. *Oilfield Rev.* **1994**, *6* (2), 33–43.
- (2) Njuguna, J.; Siddique, S.; Bakah Kwroffie, L.; Piromrat, S.; Addae-Afoakwa, K.; Ekeh-Adegbotolu, U.; Oluyemi, G.; Yates, K.; Kumar Mishra, A.; Moller, L. The Fate of Waste Drilling Fluids from Oil & Gas Industry Activities in the Exploration and Production Operations. *Waste Manage.* **2022**, *139*, 362–380.
- (3) Deville, J. P. Drilling Fluids. *Fluid Chemistry, Drilling and Completion*; Elsevier, 2022; Chapter 4. DOI: [10.1016/B978-0-12-822721-3.00010-1](https://doi.org/10.1016/B978-0-12-822721-3.00010-1).
- (4) Dvoynikov, M. V.; Nutskova, M. V.; Blinov, P. A. Developments Made in the Field of Drilling Fluids by Saint Petersburg Mining University. *Int. J. Eng., Trans. A* **2020**, *33* (4), 702–711.
- (5) Luckham, P. F.; Rossi, S. Colloidal and Rheological Properties of Bentonite Suspensions. *Adv. Colloid Interface Sci.* **1999**, *82* (1), 43–92.
- (6) Besq, A.; Malfoy, C.; Pantet, A.; Monnet, P.; Righi, D. Physicochemical Characterisation and Flow Properties of Some Bentonite Muds. *Appl. Clay Sci.* **2003**, *23* (5–6), 275–286.
- (7) ASME. *Drilling Fluids Processing Handbook*, 1st ed.; GPP, Elsevier: New York, 2005. DOI: [10.1016/B978-0-7506-7775-2.XS000-8](https://doi.org/10.1016/B978-0-7506-7775-2.XS000-8).
- (8) Caenn, R.; Chillingar, G. V. Drilling Fluids: State of the Art. *J. Pet. Sci. Eng.* **1996**, *14* (3–4), 221–230.
- (9) Kania, D.; Yunus, R.; Omar, R.; Abdul Rashid, S.; Mohamad Jan, B. A Review of Biolubricants in Drilling Fluids: Recent Research, Performance, and Applications. *J. Pet. Sci. Eng.* **2015**, *135*, 177–184.
- (10) Johanness, F. Drilling Muds. In *Petroleum Engineer's Guide to Oil Field Chemicals and Fluids*, 2nd ed.; Elsevier, 2015; pp 1–61. DOI: [10.1016/B978-0-12-803734-8.00001-1](https://doi.org/10.1016/B978-0-12-803734-8.00001-1).
- (11) Williamson, D. Defining Drilling Fluids: Drilling Fluid Basics. *Oilfield Rev.* **2013**, *25*, 63–64.
- (12) Husin, H.; Elraies, K. A.; Choi, H. J.; Aman, Z. Influence of Graphene Nanoplatelet and Silver Nanoparticle on the Rheological Properties of Water-Based Mud. *Appl. Sci.* **2018**, *8* (8), 1386.
- (13) Dolz, M.; Jiménez, J.; Hernández, M. J.; Delegido, J.; Casanovas, A. Flow and Thixotropy of Non-Contaminating Oil Drilling Fluids Formulated with Bentonite and Sodium Carboxymethyl Cellulose. *J. Pet. Sci. Eng.* **2007**, *57* (3–4), 294–302.
- (14) Khan, K.; Khan, S. A.; Saleem, M. U.; Ashraf, M. Improvement of Locally Available Raw Bentonite for Use as Drilling Mud. *Open Constr. Build. Technol. J.* **2017**, *11* (1), 274–284.
- (15) De Melo, K. C.; De Castro Dantas, T. N.; De Barros Neto, E. L. Influência Da Temperatura Na Reologia De Fluidos De Perfuração Preparados Com Carboximetilcelulose, Goma Xantana E Bentonita. *Holos* **2013**, *5*, 3.
- (16) Benyounes, K.; Mellak, A.; Benchabane, A. The Effect of Carboxymethylcellulose and Xanthan on the Rheology of Bentonite Suspensions. *Energy Sources, Part A Recover. Util. Environ. Eff.* **2010**, *32* (17), 1634–1643.
- (17) Al-Shargabi, M.; Davoodi, S.; Wood, D. A.; Al-Musai, A.; Rukavishnikov, V. S.; Minaev, K. M. Nanoparticle Applications as Beneficial Oil and Gas Drilling Fluid Additives: A Review. *J. Mol. Liq.* **2022**, *352*, 118725.
- (18) Zheng, Y.; Amiri, A.; Polycarpou, A. A. Enhancements in the Tribological Performance of Environmentally Friendly Water-Based Drilling Fluids Using Additives. *Appl. Surf. Sci.* **2020**, *527* (March), 146822.
- (19) Rafati, R.; Smith, S. R.; Sharifi Haddad, A.; Novara, R.; Hamidi, H. Effect of Nanoparticles on the Modifications of Drilling Fluids Properties: A Review of Recent Advances. *J. Pet. Sci. Eng.* **2018**, *161*, 61–76.
- (20) Farahbod, F. Experimental Investigation of Thermo-Physical Properties of Drilling Fluid Integrated with Nanoparticles: Improvement of Drilling Operation Performance. *Powder Technol.* **2021**, *384*, 125–131.
- (21) Hemmat Esfe, M.; Bahiraei, M.; Mir, A. Application of Conventional and Hybrid Nanofluids in Different Machining Processes: A Critical Review. *Adv. Colloid Interface Sci.* **2020**, *282*, 102199.
- (22) Agarwal, S.; Tran, P.; Song, Y.; Martello, D.; Gupta, R. K. Flow Behavior of Nanoparticle Stabilized Drilling Fluids and Effect of High Temperature Aging. *2011 AADE National Technical Conference and Exhibition*; American Association of Drilling Engineers (AADE), 2016; Vol. 4, pp 1–23.

- (23) Cheraghian, G. G.; Afrand, M. Nanotechnology for Drilling Operations. *Emergency Nanotechnologies for Renewable Energy* **2021**, 135–148.
- (24) Cheraghian, G. Nanoparticles in Drilling Fluid: A Review of the State-of-the-Art. *J. Mater. Res. Technol.* **2021**, 13, 737–753.
- (25) Novara, R.; Rafati, R.; Sharifi Haddad, A. Rheological and Filtration Property Evaluations of the Nano-Based Muds for Drilling Applications in Low Temperature Environments. *Colloids Surf. A: Physicochem. Eng. Asp.* **2021**, 622 (March), 126632.
- (26) Vryzas, Z.; Kelessidis, V. C. Nano-Based Drilling Fluids: A Review. *Energies* **2017**, 10 (4), 540.
- (27) Friedheim, J.; Young, S.; De Stefano, G.; Lee, J.; Guo, Q. Nanotechnology for Oilfield Applications - Hype or Reality?. *SPE International Oilfield Nanotechnology Conference and Exhibition*; Society of Petroleum Engineers, 2012; pp 304–310. .
- (28) Baig, N.; Kammakakam, I.; Falath, W. Nanomaterials: A Review of Synthesis Methods, Properties, Recent Progress, and Challenges. *Mater. Adv.* **2021**, 2 (6), 1821–1871.
- (29) Kolahalam, L. A.; Kasi Viswanath, I. V.; Diwakar, B. S.; Govindh, B.; Reddy, V.; Murthy, Y. L. N. Review on Nanomaterials: Synthesis and Applications. *Mater. Today Proc.* **2019**, 18, 2182–2190.
- (30) Lead, J. R.; Batley, G. E.; Alvarez, P. J. J.; Croteau, M. N.; Handy, R. D.; McLaughlin, M. J.; Judy, J. D.; Schirmer, K. Nanomaterials in the Environment: Behavior, Fate, Bioavailability, and Effects—An Updated Review. *Environ. Toxicol. Chem.* **2018**, 37 (8), 2029–2063.
- (31) Magne, T. M.; de Oliveira Vieira, T.; Costa, B.; Alencar, L. M. R.; Ricci-Junior, E.; Hu, R.; Qu, J.; Zamora-Ledezma, C.; Alexis, F.; Santos-Oliveira, R. Factors Affecting the Biological Response of Graphene. *Colloids Surfaces B: Biointerfaces* **2021**, 203, 111767.
- (32) Zamora-Ledezma, C.; Chicaiza-Zambrano, A.; Santiago Vispo, N.; Debut, A.; Vizuete, K.; Guerrero, V. H.; Almeida, C. E.; Alexis, F. Frequency Based Control of Antifouling Properties Using Graphene Nanoplatelet/Poly(Lactic-Co-Glycolic Acid) Composite Films. *Compos. Interfaces* **2021**, 28 (11), 1137–1153.
- (33) Torres-Canas, F. J.; Blanc, C.; Zamora-Ledezma, C.; Silva, P.; Anglaret, E. Dispersion and Individualization of SWNT in Surfactant-Free Suspensions and Composites of Hydrosoluble Polymers. *J. Phys. Chem. C* **2015**, 119 (1), 703–709.
- (34) Suppan, G.; Briones-Macias, M.; Pazmiño-Arias, E.; Zamora-Ledezma, C. Fabrication and Characterization of Metal-Free Composite Electrodes Based on Few-Layer-Graphene Nanoplatelets for Oxygen Reduction Reaction Applications. *Phys. status solidi* **2021**, 258, 2000515.
- (35) González, A. L.; Noguez, C.; Beránek, J.; Barnard, A. S. Size, Shape, Stability, and Color of Plasmonic Silver Nanoparticles. *J. Phys. Chem. C* **2014**, 118 (17), 9128–9136.
- (36) Peng, Z.; Liu, X.; Zhang, W.; Zeng, Z.; Liu, Z.; Zhang, C.; Liu, Y.; Shao, B.; Liang, Q.; Tang, W.; Yuan, X. Advances in the Application, Toxicity and Degradation of Carbon Nanomaterials in Environment: A Review. *Environ. Int.* **2020**, 134, 105298.
- (37) Ikram, R.; Jan, B. M.; Vejpravova, J. Towards Recent Tendencies in Drilling Fluids: Application of Carbon-Based Nanomaterials. *J. Mater. Res. Technol.* **2021**, 15, 3733–3758.
- (38) Rafieefar, A.; Sharif, F.; Hashemi, A.; Bazargan, A. M. Rheological Behavior and Filtration of Water-Based Drilling Fluids Containing Graphene Oxide: Experimental Measurement, Mechanistic Understanding, and Modeling. *ACS Omega* **2021**, 6 (44), 29905–29920.
- (39) Liu, S.; Yao, F.; Kang, M.; Zhao, S.; Huang, Q.; Fu, G. Hierarchical Xanthan Gum/Graphene Oxide Nanocomposite Film Induced by Ferric Ions Coordination. *Mater. Des.* **2017**, 113, 232–239.
- (40) Ismail, A. R.; Aftab, A.; Ibupoto, Z. H.; Zolkifile, N. The Novel Approach for the Enhancement of Rheological Properties of Water-Based Drilling Fluids by Using Multi-Walled Carbon Nanotube, Nanosilica and Glass Beads. *J. Pet. Sci. Eng.* **2016**, 139, 264–275.
- (41) Taha, N. M.; Lee, S. Nano Graphene Application Improving Drilling Fluids Performance. *International Petroleum Technology Conference*; IPTC, 2015; pp 6–9. DOI: 10.2523/IPTC-18539-MS.
- (42) Kosynkin, D. V.; Ceriotti, G.; Wilson, K. C.; Lomeda, J. R.; Scorsone, J. T.; Patel, A. D.; Friedheim, J. E.; Tour, J. M. Graphene Oxide as a High-Performance Fluid-Loss-Control Additive in Water-Based Drilling Fluids. *ACS Appl. Mater. Interfaces* **2012**, 4 (1), 222–227.
- (43) Samsuri, A.; Hamzah, A. Water Based Mud Lifting Capacity Improvement by Multiwall Carbon Nanotubes Additive. *J. Pet. Gas Eng.* **2011**, 2 (5), 99–107.
- (44) Torres-Canas, F.; Blanc, C.; Mašlík, J.; Tahir, S.; Izard, N.; Karasahin, S.; Castellani, M.; Dammasch, M.; Zamora-Ledezma, C.; Anglaret, E. Morphology and Anisotropy of Thin Conductive Inkjet Printed Lines of Single-Walled Carbon Nanotubes. *Mater. Res. Express* **2017**, 4 (3), 035037.
- (45) William, J. K. M.; Ponmani, S.; Samuel, R.; Nagarajan, R.; Sangwai, J. S. Effect of CuO and ZnO Nanofluids in Xanthan Gum on Thermal, Electrical and High Pressure Rheology of Water-Based Drilling Fluids. *J. Pet. Sci. Eng.* **2014**, 117, 15–27.
- (46) Beg, M.; Kumar, P.; Choudhary, P.; Sharma, S. Effect of High Temperature Ageing on TiO<sub>2</sub> Nanoparticles Enhanced Drilling Fluids: A Rheological and Filtration Study. *Upstream Oil Gas Technol.* **2020**, S, 100019.
- (47) Gallardo, F. E.; Erdmann, E.; Abalos, R. Evaluación Reológica de Fluidos de Perforación Base Agua Con Nanosilíce. *Materia (Rio de Janeiro)* **2018**, 23 (2). DOI: 10.1590/S1517-707620180002.0470.
- (48) Perween, S.; Thakur, N. K.; Beg, M.; Sharma, S.; Ranjan, A. Enhancing the Properties of Water Based Drilling Fluid Using Bismuth Ferrite Nanoparticles. *Colloids Surfaces A: Physicochem. Eng. Asp.* **2019**, 561, 165–177.
- (49) Hong, S. H.; Jo, H. J.; Choi, M. J.; Jang, H. W.; Kim, Y. J.; Hwang, W. R.; Kim, S. Y. Influence of MoS<sub>2</sub> Nanosheet Size on Performance of Drilling Mud. *Polymers (Basel)*. **2019**, 11 (2), 321.
- (50) Xiao, H.; Liu, S. 2D Nanomaterials as Lubricant Additive: A Review. *Mater. Des.* **2017**, 135, 319–332.
- (51) Borisov, A. S.; Husein, M.; Hareland, G. A Field Application of Nanoparticle-Based Invert Emulsion Drilling Fluids. *J. Nanopart. Res.* **2015**, 17 (8), 340.
- (52) Zhou, G.; Qiu, Z.; Zhong, H.; Zhao, X.; Kong, X. Study of Environmentally Friendly Wild Jujube Pit Powder as a Water-Based Drilling Fluid Additive. *ACS Omega* **2021**, 6 (2), 1436–1444.
- (53) Wan, K.; Li, Y.; Wang, Y.; Wei, G. Recent Advance in the Fabrication of 2D and 3D Metal Carbides-Based Nanomaterials for Energy and Environmental Applications. *Nanomaterials* **2021**, 11 (1), 246.
- (54) Liu, Y. Field Tests of High-Density Oil-Based Drilling Fluid Application in Horizontal Segment. *Nat. Gas Ind. B* **2021**, 8 (3), 231–238.
- (55) Ozkan, A. Effect of Gold Nanoparticle Functionalized Multi-Walled Carbon Nanotubes on the Properties of Na-Bentonite Water Based Drilling Fluid. *Fresenius Environ. Bull.* **2020**, 29 (1), 143–151.
- (56) Ismail, A. R.; Rashid, N. M.; Jaafar, M. Z.; Sulaiman, W. R. W.; Buang, N. A. Effect of Nanomaterial on the Rheology of Drilling Fluids. *J. Appl. Sci.* **2014**, 14 (11), 1192–1197.
- (57) Saffari, H. R. M.; Soltani, R.; Alaei, M.; Soleymani, M. Tribological Properties of Water-Based Drilling Fluids with Borate Nanoparticles as Lubricant Additives. *J. Pet. Sci. Eng.* **2018**, 171 (July), 253–259.
- (58) Kazemi-Beydokhti, A.; Hajiabadi, S. H. Rheological Investigation of Smart Polymer/Carbon Nanotube Complex on Properties of Water-Based Drilling Fluids. *Colloids Surf. A Physicochem. Eng. Asp.* **2018**, 556, 23–29.
- (59) Zhang, H. Ultrathin Two-Dimensional Nanomaterials. *ACS Nano* **2015**, 9 (10), 9451–9469.
- (60) Shao, J. J.; Raidongia, K.; Koltonow, A. R.; Huang, J. Self-Assembled Two-Dimensional Nanofluidic Proton Channels with High Thermal Stability. *Nat. Commun.* **2015**, 6 (May), 1–7.
- (61) Koski, K. J.; Cui, Y. The New Skinny in Two-Dimensional Nanomaterials. *ACS Nano* **2013**, 7 (5), 3739–3743.
- (62) Wan, Y.; Fan, Y.; Dan, J.; Hong, C.; Yang, S.; Yu, F. A Review of Recent Advances in Two-Dimensional Natural Clay Vermiculite-Based Nanomaterials. *Mater. Res. Express* **2019**, 6 (10), 102002.

- (63) Liu, F.; Jiang, G. C.; Wang, K.; Wang, J. Laponite Nanoparticle as a Multi-Functional Additive in Water-Based Drilling Fluids. *J. Mater. Sci.* **2017**, *52* (20), 12266–12278.
- (64) Zhuang, G.; Zhang, Z.; Jaber, M.; Gao, J.; Peng, S. Comparative Study on the Structures and Properties of Organo-Montmorillonite and Organo-Palygorskite in Oil-Based Drilling Fluids. *J. Ind. Eng. Chem.* **2017**, *56*, 248–257.
- (65) *Specification for Drilling-Fluid Materials*, API Specification 13A; American Petroleum Institute, 1993; p 52.
- (66) *Recommended Practice for Field Testing Water-Based Drilling Fluids*, API Specification 13B-1; American Petroleum Institute, 2017; p 121.
- (67) Farjadian, F.; Abbaspour, S.; Sadatlu, M. A. A.; Mirkiani, S.; Ghasemi, A.; Hoseini-Ghahfarokhi, M.; Mozaffari, N.; Karimi, M.; Hamblin, M. R. Recent Developments in Graphene and Graphene Oxide: Properties, Synthesis, and Modifications: A Review. *ChemistrySelect* **2020**, *5* (33), 10200–10219.
- (68) Mohan, V. B.; Lau, K. ta.; Hui, D.; Bhattacharyya, D. Graphene-Based Materials and Their Composites: A Review on Production, Applications and Product Limitations. *Compos. Part B: Eng.* **2018**, *142*, 200–220.
- (69) Mei, S.; Yang, J.; Ferreira, J. M. F. Comparison of Dispersants Performance in Slip Casting of Cordierite-Based Glass-Ceramics. *Ceram. Int.* **2003**, *29* (7), 785–791.
- (70) Wang, S.; Shu, Z.; Chen, L.; Yan, P.; Li, B.; Yuan, C.; Jian, L. Low Temperature Green Nano-Composite Vegetable-Gum Drilling Fluid. *Appl. Nanosci.* **2019**, *9* (7), 1579–1591.
- (71) Huang, X. Bi.; Sun, J. S.; Huang, Y.; Yan, B. C.; Dong, X. D.; Liu, F.; Wang, R. Laponite: A Promising Nanomaterial to Formulate High-Performance Water-Based Drilling Fluids. *Pet. Sci.* **2021**, *18* (2), 579–590.
- (72) Ma, J.; Pang, S.; Zhang, Z.; Xia, B.; An, Y. Experimental Study on the Polymer/Graphene Oxide Composite as a Fluid Loss Agent for Water-Based Drilling Fluids. *ACS Omega* **2021**, *6* (14), 9750–9763.
- (73) Hajiabadi, S. H.; Aghaei, H.; Ghabdian, M.; Kalateh-Aghamohammadi, M.; Esmailnezhad, E.; Choi, H. J. On the Attributes of Invert-Emulsion Drilling Fluids Modified with Graphene Oxide/Inorganic Complexes. *J. Ind. Eng. Chem.* **2021**, *93*, 290–301.
- (74) Alvi, M. A. A.; Belayneh, M.; Saasen, A.; Aadnøy, B. S. The Effect of Micro-Sized Boron Nitride BN and Iron Trioxide Fe<sub>2</sub>O<sub>3</sub> Nanoparticles on the Properties of Laboratory Bentonite Drilling Fluid. *SPE Norway One Day Seminar*; Society of Petroleum Engineers, 2018; pp 478–491.
- (75) Wrobel, S. Effect Of MoS<sub>2</sub>- and Graphene Nanoparticles on the Properties & Performance of Polymer/Salt Treated Bentonite Drilling Fluid. *Int. J. NanoSci. Nanotechnol.* **2017**, *8* (1), 59–71.
- (76) Kang, J.; Sangwan, V. K.; Wood, J. D.; Hersam, M. C. Solution-Based Processing of Monodisperse Two-Dimensional Nanomaterials. *Acc. Chem. Res.* **2017**, *50* (4), 943–951.
- (77) Rasool, M. H.; Zamir, A.; Ahmed, M.; Stephen, S. E. A Study on The Effects of Temperature, Salinity and PH on the Rheological Behavior of Water Based Mud (WBM) with Graphene Nanoparticles. *Conference Proceedings: FYP & Postgraduate Poster Competition*, 2020; pp 48–53.
- (78) Ibrahim, A.; Ridha, S.; Amer, A.; Shahari, R.; Ganat, T. Influence of Degree of Dispersion of Noncovalent Functionalized Graphene Nanoplatelets on Rheological Behaviour of Aqueous Drilling Fluids. *Int. J. Chem. Eng.* **2019**, *2019*, 8107168.
- (79) Ma, L.; Xie, G.; Luo, P.; Zhang, L.; Fan, Y.; He, Y. Dispersion Stability of Graphene Oxide in Extreme Environments and Its Applications in Shale Exploitation. *ACS Sustain. Chem. Eng.* **2022**, *10* (8), 2609–2623.
- (80) Gholami, R.; Raza, A.; Rabiei, M.; Fakhari, N.; Balasubramaniam, P.; Rasouli, V.; Nagarajan, R. An Approach to Improve Wellbore Stability in Active Shale Formations Using Nanomaterials. *Petroleum* **2021**, *7* (1), 24–32.
- (81) Xiong, Z.; Fu, F.; Li, X. Experimental Investigation on Laponite as Ultra-High-Temperature Viscosifier of Water-Based Drilling Fluids. *SN Appl. Sci.* **2019**, *1* (11), 1–8.
- (82) Medhi, S.; Chowdhury, S.; Bhatt, N.; Gupta, D. K.; Rana, S.; Sangwai, J. S. Analysis of High Performing Graphene Oxide Nanosheets Based Non-Damaging Drilling Fluids through Rheological Measurements and CFD Studies. *Powder Technol.* **2021**, *377*, 379–395.
- (83) Karakosta, K.; Mitropoulos, A. C.; Kyzas, G. Z. A Review in Nanopolymers for Drilling Fluids Applications. *J. Mol. Struct.* **2021**, *1227*, 129702.
- (84) Baba Hamed, S.; Belhadri, M. Rheological Properties of Biopolymers Drilling Fluids. *J. Pet. Sci. Eng.* **2009**, *67* (3–4), 84–90.
- (85) Elkatatny, S. Enhancing the Rheological Properties of Water-Based Drilling Fluid Using Micronized Starch. *Arab. J. Sci. Eng.* **2019**, *44* (6), 5433–5442.
- (86) Delikeshva, D. N.; Syzdykov, A. K.; Ismailova, J. A.; Kabdushev, A. A.; Bukayeva, G. A. Measurement of the Plastic Viscosity and Yield Point of Drilling Fluids. *Int. J. Eng. Res. Technol.* **2020**, *13* (1), 58–65.
- (87) Maiti, M.; Ranjan, R.; Chaturvedi, E.; Bhaumik, A. K.; Mandal, A. Formulation and Characterization of Water-Based Drilling Fluids for Gas Hydrate Reservoirs with Efficient Inhibition Properties. *J. Dispers. Sci. Technol.* **2021**, *42* (3), 338–351.
- (88) Gudarzifar, H.; Sabbaghi, S.; Rezvani, A.; Saboori, R. Experimental Investigation of Rheological & Filtration Properties and Thermal Conductivity of Water-Based Drilling Fluid Enhanced. *Powder Technol.* **2020**, *368*, 323–341.
- (89) Belayneh, M.; Aadnøy, B.; Strømø, S. M. MoS<sub>2</sub> Nanoparticle Effects on 80 °C Thermally Stable Water-Based Drilling Fluid. *Materials (Basel)* **2021**, *14* (23), 7195.
- (90) Perumalsamy, J.; Gupta, P.; Sangwai, J. S. Performance Evaluation of Esters and Graphene Nanoparticles as an Additives on the Rheological and Lubrication Properties of Water-Based Drilling Mud. *J. Pet. Sci. Eng.* **2021**, *204* (March), 108680.
- (91) Mezger, T. G. *The Rheology Handbook*, 4th ed.; Vincentz, 2014. DOI: 10.1108/prt.2009.12938eac.006.
- (92) Poulin, P.; Jalili, R.; Neri, W.; Nallet, F.; Divoux, T.; Colin, A.; Aboutaleb, S. H.; Wallace, G.; Zakri, C. Superflexibility of Graphene Oxide. *Proc. Natl. Acad. Sci. U. S. A.* **2016**, *113* (40), 11088–11093.
- (93) Liu, F.; Jiang, G. C.; Wang, K.; Wang, J. X. Laponite Nanoparticle as a High Performance Rheological Modifier in Water-Based Drilling Fluids. *Mater. Sci. Forum* **2018**, *917*, 134–139.
- (94) Ikram, R.; Mohamed Jan, B.; Sidek, A.; Kenanakis, G. Utilization of Eco-Friendly Waste Generated Nanomaterials in Water-Based Drilling Fluids; State of the Art Review. *Materials (Basel)*. **2021**, *14* (15), 4171.
- (95) Temraz, M. G.; Hassanien, I. Mineralogy and Rheological Properties of Some Egyptian Bentonite for Drilling Fluids. *J. Nat. Gas Sci. Eng.* **2016**, *31*, 791–799.
- (96) Villar, M. V.; Iglesias, R. J.; García-Siñeriz, J. L.; Lloret, A.; Huertas, F. Physical Evolution of a Bentonite Buffer during 18 Years of Heating and Hydration. *Eng. Geol.* **2020**, *264*, 105408.
- (97) Alcheikh, I. M.; Ghosh, B. A Comprehensive Review on the Advancement of Non-Damaging Drilling Fluids. *Int. J. Petrochemistry Res.* **2017**, *1* (1), 61–72.
- (98) Li, W.; Jiang, G.; Ni, X.; Li, Y.; Wang, X.; Luo, X. Styrene Butadiene Resin/Nano-SiO<sub>2</sub> Composite as a Water-and-Oil-Dispersible Plugging Agent for Oil-Based Drilling Fluid. *Colloids Surfaces A Physicochem. Eng. Asp.* **2020**, *606* (June), 125245.
- (99) Terrones, M.; Botello-Méndez, A. R.; Campos-Delgado, J.; López-Urías, F.; Vega-Cantú, Y. L.; Rodríguez-Macías, F. J.; Elías, A. L.; Muñoz-Sandoval, E.; Cano-Márquez, A. G.; Charlier, J. C.; Terrones, H. Graphene and Graphite Nanoribbons: Morphology, Properties, Synthesis, Defects and Applications. *Nano Today* **2010**, *5* (4), 351–372.
- (100) Maiti, M.; Bhaumik, A. K.; Mandal, A. Performance of Water-Based Drilling Fluids for Deepwater and Hydrate Reservoirs: Designing and Modelling Studies. *Pet. Sci.* **2021**, *18* (6), 1709–1728.
- (101) Razi, M. M.; Ghiass, M.; Razi, F. M. Effect of Guar Gum Polymer and Lime Powder Addition on the Fluid Loss and Rheological Properties of the Bentonite Dispersions. *J. Dispers. Sci. Technol.* **2013**, *34* (5), 731–736.

- (102) Aramendiz, J.; Imqam, A. Water-Based Drilling Fluid Formulation Using Silica and Graphene Nanoparticles for Unconventional Shale Applications. *J. Pet. Sci. Eng.* **2019**, *179*, 742–749.
- (103) Wang, K.; Jiang, G.; Liu, F.; Yang, L.; Ni, X.; Wang, J. Magnesium Aluminum Silicate Nanoparticles as a High-Performance Rheological Modifier in Water-Based Drilling Fluids. *Appl. Clay Sci.* **2018**, *161* (March), 427–435.
- (104) Huang, X.; Lv, K.; Sun, J.; Lu, Z.; Bai, Y.; Shen, H.; Wang, J. Enhancement of Thermal Stability of Drilling Fluid Using Laponite Nanoparticles under Extreme Temperature Conditions. *Mater. Lett.* **2019**, *248*, 146–149.
- (105) Movahedi, H.; Jamshidi, S.; Hajipour, M. New Insight into the Filtration Control of Drilling Fluids Using a Graphene-Based Nanocomposite under Static and Dynamic Conditions. *ACS Sustain. Chem. Eng.* **2021**, *9* (38), 12844–12857.
- (106) Lalji, S. M.; Khan, M. A.; Haneef, J.; Ali, S. I.; Arain, A. H.; Shah, S. S. Nano-particles Adapted Drilling Fluids for the Swelling Inhibition for the Northern Region Clay Formation of Pakistan. *Appl. Nanosci.* **2021**.
- (107) Alvarado, D. A.; Marsden, S. S. Flow of Oil-in-Water Emulsions Through Tubes and Porous Media. *Soc. Pet. Eng. AIME J.* **1979**, *19* (6), 369–377.
- (108) Alvarado, V.; Manrique, E. Enhanced Oil Recovery: An Update Review. *Energies* **2010**, *3* (9), 1529–1575.
- (109) Irfan, S. A.; Shafie, A.; Yahya, N.; Zainuddin, N. Mathematical Modeling and Simulation of Nanoparticle-Assisted Enhanced Oil Recovery - A Review. *Energies* **2019**, *12* (8), 1575.
- (110) Wood, B. D.; He, X.; Apte, S. V. Modeling Turbulent Flows in Porous Media. *Annu. Rev. Fluid Mech.* **2020**, *52*, 171–203.
- (111) Zakirov, T. R.; Khramchenkov, M. G. Pore-Scale Study of the Anisotropic Effect on Immiscible Displacement in Porous Media under Different Wetting Conditions and Capillary Numbers. *J. Pet. Sci. Eng.* **2022**, *208* (PB), 109484.
- (112) Lyubimova, T.; Ivantsov, A.; Lyubimov, D. Control of Fingering Instability by Vibrations. *Math. Model. Nat. Phenom.* **2021**, *16*, 40.
- (113) Zhang, X.; Wang, L.; Zhu, H.; Zeng, C. Pore-Scale Simulation of Salt Fingers in Porous Media Using a Coupled Iterative Source-Correction Immersed Boundary-Lattice Boltzmann Solver. *Appl. Math. Model.* **2021**, *94*, 656–675.
- (114) Durlafsky, L.; Brady, J. F.; Bossis, G. Dynamic Simulation of Hydrodynamically Interacting Particles. *J. Fluid Mech.* **1987**, *180*, 21–49.
- (115) *Hybrid Enhanced Oil Recovery Processes for Heavy Oil Reservoirs*, 1st ed.; Dong, X., Liu, H., Chen, Z., Eds.; Elsevier, 2021.
- (116) Bensimon, D.; Kadanoff, L. P.; Liang, S.; Shraiman, B. I.; Tang, C. Viscous Flows in Two Dimensions. *Rev. Mod. Phys.* **1986**, *58* (4), 977–999.
- (117) Mclean, J. W.; Saffman, P. G. The Effect of Surface Tension on the Shape of Fingers in a Hele Shaw Cell. *J. Fluid Mech.* **1981**, *102*, 455–469.
- (118) Guillen, V. R.; Carvalho, M. S.; Alvarado, V. Pore Scale and Macroscopic Displacement Mechanisms in Emulsion Flooding. *Transp. Porous Media* **2012**, *94* (1), 197–206.
- (119) Cobos, S.; Carvalho, M. S.; Alvarado, V. Flow of Oil-Water Emulsions through a Constricted Capillary. *Int. J. Multiph. Flow* **2009**, *35* (6), 507–515.
- (120) Rabbani, H. S.; Or, D.; Liu, Y.; Lai, C. Y.; Lu, N. B.; Datta, S. S.; Stone, H. A.; Shokri, N. Suppressing Viscous Fingering in Structured Porous Media. *Proc. Natl. Acad. Sci. U. S. A.* **2018**, *115* (19), 4833–4838.
- (121) Al-Housseiny, T. T.; Tsai, P. A.; Stone, H. A. Control of Interfacial Instabilities Using Flow Geometry. *Nat. Phys.* **2012**, *8* (10), 747–750.
- (122) Eslami, A.; Basak, R.; Taghavi, S. M. Multiphase Viscoplastic Flows in a Nonuniform Hele-Shaw Cell: A Fluidic Device to Control Interfacial Patterns. *Ind. Eng. Chem. Res.* **2020**, *59* (9), 4119–4133.
- (123) Mirzadeh, M.; Bazant, M. Z. Electrokinetic Control of Viscous Fingering. *Phys. Rev. Lett.* **2017**, *119*, 174501.
- (124) Angulo, R. F.; Medina, E. Conductance Distributions in Random Resistor Networks. Self-Averaging and Disorder Lengths. *J. Stat. Phys.* **1994**, *75*, 135–151.
- (125) García, X.; Araujo, M.; Medina, E. P-Wave Velocity - Porosity Relations and Homogeneity Lengths in a Realistic Deposition Model of Sedimentary Rock. *Waves in Random Media* **2004**, *14*, 129–142.
- (126) León, D. Interphase Analysis of Viscous Flow in Porous Media to Enhance Oil Recovery. Bachelor's Thesis, Yachay Tech University, Ucuqui, Ecuador, 2021.
- (127) Espanol, P.; Warren, P. Statistical Mechanics of Dissipative Particle Dynamics. *EPL* **1995**, *30* (4), 191–196.
- (128) Koelman, J. M. V. A.; Hoogerbrugge, P. J. Dynamic Simulations of Hard-Sphere Suspensions under Steady Shear. *EPL* **1993**, *21* (3), 363–368.
- (129) Hoogerbrugge, P. J.; Koelman, J. M. V. A. Simulating Microscopic Hydrodynamic Phenomena with Dissipative Particle Dynamics. *EPL* **1992**, *19* (3), 155–160.
- (130) Goga, N.; Rzepiela, A. J.; De Vries, A. H.; Marrink, S. J.; Berendsen, H. J. C. Efficient Algorithms for Langevin and DPD Dynamics. *J. Chem. Theory Comput.* **2012**, *8* (10), 3637–3649.
- (131) Gingold, R. A.; Monaghan, J. J. Smoothed Particle Hydrodynamics: Theory and Application to Non-Spherical Stars. *Mon. Not. R. Astron. Soc.* **1977**, *181*, 375–389.
- (132) Meakin, P.; Xu, Z. Dissipative Particle Dynamics and Other Particle Methods for Multiphase Fluid Flow in Fractured and Porous Media. *Prog. Comput. Fluid Dyn.* **2009**, *9* (6-7), 399–408.
- (133) Li, Y.; Li, X.; Li, Z.; Gao, H. Surface-Structure-Regulated Penetration of Nanoparticles across a Cell Membrane. *Nanoscale* **2012**, *4*, 3768–3775.
- (134) Osher, S.; Sethian, J. Fronts Propagating with Curvature-Dependent Speed: Algorithms Based on Hamilton-Jacobi Formulations. *J. Comput. Phys.* **1988**, *79*, 12–49.
- (135) Frisch, U.; Hasslacher, B.; Pomeau, Y. Lattice-Gas Automata for the Navier-Stokes Equation. *Phys. Rev. Lett.* **1986**, *56* (14), 1505–1508.
- (136) Wolfram, S. Statistical Mechanics of Cellular Automata. *Rev. Mod. Phys.* **1983**, *55* (3), 601–644.
- (137) Chen, S.; Doolen, G. D. Lattice Boltzmann Method for Fluid Flows. *Annu. Rev. Fluid Mech.* **1998**, *30*, 329–364.
- (138) Schornbaum, F.; Rude, U. Massively Parallel Algorithms for the Lattice Boltzmann Method on Nonuniform Grids. *SIAM J. Sci. Comput.* **2016**, *38* (2), C96–C126.
- (139) Chen, Y.; Teng, S.; Shukuwa, T.; Ohashi, H. Lattice-Boltzmann Simulation of Two-Phase Fluid Flows. *Int. J. Mod. Phys. C* **1998**, *9* (8), 1383–1391.
- (140) Kupershtokh, A. L.; Medvedev, D. A.; Gribanov, I. I. Thermal Lattice Boltzmann Method for Multiphase Flows. *Phys. Rev. E* **2018**, *98* (2), 023308.
- (141) Hedjripour, A. H.; Callaghan, D. P.; Baldock, T. E. Generalized Transformation of the Lattice Boltzmann Method for Shallow Water Flows. *J. Hydraul. Res.* **2016**, *54* (4), 371–388.
- (142) Liu, H.; Zhang, Y.; Valocchi, A. J. Lattice Boltzmann Simulation of Immiscible Fluid Displacement in Porous Media: Homogeneous versus Heterogeneous Pore Network. *Phys. Fluids* **2015**, *27*, 052103.